REPRESSION OF HIGH VELOCITY FLOW PHENOMENA AROUND SHARP BENDS IN SUPER-CRITICALLY SLOPED OPEN CHANNELS

Thesis by

Warren O. Wagner

Submitted in Partial Fulfillment of the Requirements
for the Degree of Doctor of Philosophy

California Institute of Technology
Pasadena, California

1945

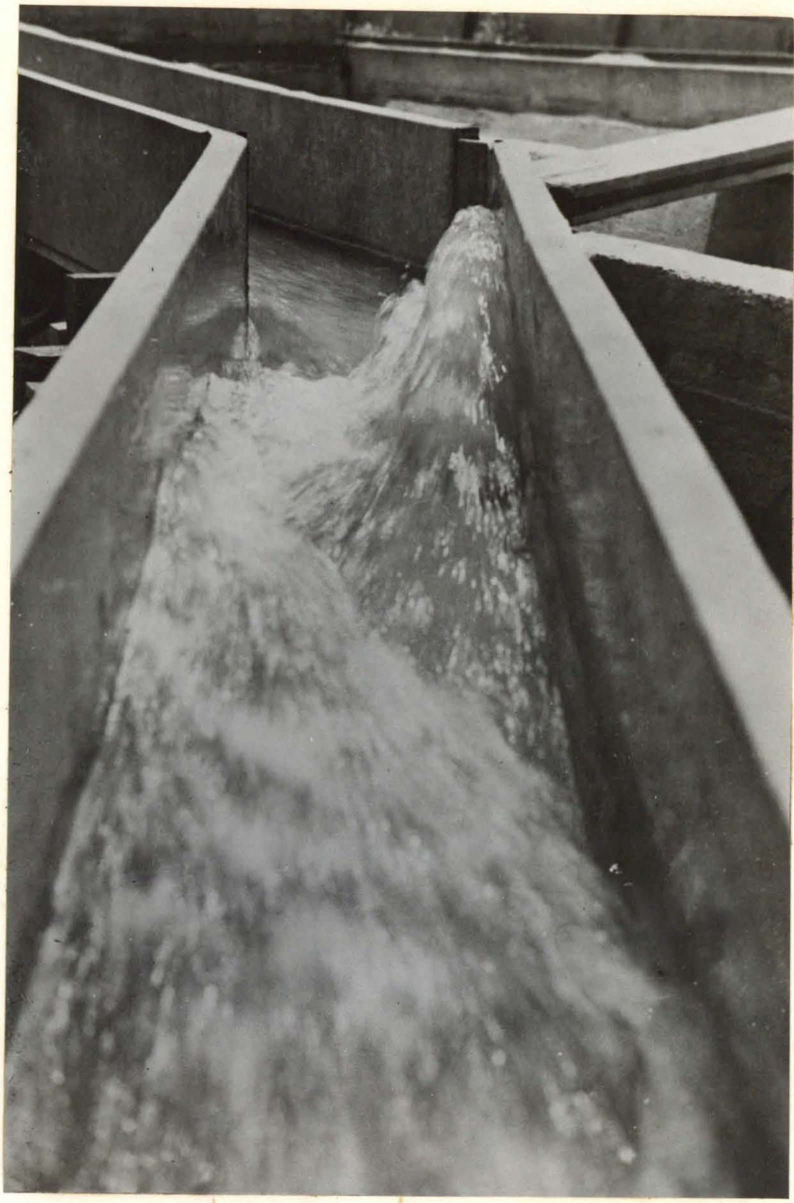

THE PROBLEM

Analysis and Repression of These Waves

TABLE OF CONTENTS

PART I.

INTRODUCTION

PART II.

ANALYTICAL STUDY

PART III.

EXPERIMENTAL STUDY

PART IV.

COMPARISON OF ANALYTICAL AND EXPERIMENTAL RESULTS

PART V.

CONCLUSIONS

APPENDIX

I. SUMMARY AND INTRODUCTION

A. SUMMARY

This investigation was conducted for the purpose of contributing additional information to our present knowledge of the principles of super-critical flow around bends in open channels. The effects of a mild but abrupt bend in a steeply sloped channel were studied and numerous experiments were made with various types of control devices designed to repress the undesirable waves created by the bend.

The channel used for these experiments was 18 inches wide, 12 inches deep, and approximately 40 feet long, with a 10° abrupt bend at its mid-point. Measurements were made of wave heights along the walls and over the water surface, of velocities and their changes (both in magnitude and direction) from section to section, and of forces acting due to the consequent changes in momentum.

The experimental results obtained agree well with the analytical developments propounded. Wall wave heights above those for uniform flow were reduced by the proper control device to as little as one-third the wave heights created by the bend in the untreated channel, with the accompanying establishment of fairly uniform conditions of velocity and cross-sectional area below the control device. With such satisfactory repression of the undesirable waves in a single, small-angle abrupt bend, it is felt that the principle could be extended to a large angle bend by using a series of these small, abrupt bends one below another.

B. NOTATION

α = angle of sill with upstream channel

β = wave angle

b = width of channel (= 1.50 feet)

C = wave celerity

CB = center of bend

d = depth of water in channel

d_1 = uniform upstream depth

d_2 = depth beyond wave front or downstream depth

d_c = critical depth

$D\text{-}x$ = distance x downstream from bend

E = specific energy

F = Froude Number = $V_1/\sqrt{gd_1}$

g = gravity constant

h = height of sill

IW = inside wall of channel

J = force divided by mass of water flowing per second

ℓ = length of sill

L = wave length

n = coefficient of friction for channel (n = 0.0085)

OW = outside wall

P = force

ϕ = effective turning angle exerted by sills

Q = discharge in cu.ft. per sec.

R = radius of curvature in curved channels.

R_{out} = location of first cross-wave on outside wall

R_{in} = location of first cross-wave on inside wall

S = bottom slope of channel

θ = angle of bend

$U-x$ = distance x upstream from bend

V = velocity in feet per second

V_1 = upstream velocity in feet per second

w = specific weight of water

W = rate of discharge in lbs. per sec.

C. INTRODUCTION AND STATEMENT OF PROBLEM

Many sections of the United States are subject to occasional and infrequent rainfalls of intense magnitudes, while in normal years the rainfall may be so minor as to cause only a small flow in the adjoining streams and their tributaries. In the central, eastern, and northern parts of the United States most rivers flow at a substantial rate throughout the year, being fed principally from areas covered by snow for a portion of the year. In the south-western portion of our country, however, rivers may flow for only a few days annually, at other times completely drying up so far as surface flow is concerned. Such a condition is found in many portions of Southern California and parts of Nevada, Arizona, New Mexico, and Texas.

With little or no water flowing for most of the days of the year, there is a natural tendency on the part of a densely populated area to encroach more and more upon the banks of the streams, confining the river channels to smaller and smaller areas just sufficiently large to handle the normal yearly flood flows. When the slope of the river drainage bed is mild, this encroachment can be greatly counteracted by deeper excavation of the channel and by providing a smoother bottom and side walls. However, when the slope is steep, this corrective method is prohibitive because of the excessive cost of confining the flow within the channel walls.

Flow phenomena on steep slopes is entirely different from that on mild slopes. As long as the flow continues without change in direction, no appreciable physical difference in the two types of flow occurs. It is comparatively inexpensive to confine the flow within the channel walls around a bend where the slope is mild, but it is quite a different problem where the slope is steep. Waves build up along the walls of the channel at the bend and downstream from it, which may become several times the depth of the normal flow. These conditions of high velocity flow occur elsewhere as well, so that a study of such flow is not confined to flood channels, although the need for a remedy is most apparent in such channels.

Practically no information was available on high velocity flow around bends in open channels until the publication of the results of a test conducted by Knapp and Ippen[1] on the flow around curves in rectangular channels. Their results proved so satisfactory and so entirely different from any previously anticipated results that their research was continued in the attempt to find some means for diminishing the dangerous, high wall waves[2]. This latter study also included flow in a trapezoidal-shaped channel.

The problem dealt with in the investigation presented, herewith, had to do with flow around a sharp bend and possible means of repressing undesirable features of the flow created by the bend.

1 Subscripts refer to material listed in the bibliography.

II. ANALYTICAL STUDY

A. REVIEW OF PROPERTIES OF HIGH VELOCITY FLOW

The term "specific energy" was first introduced by Bakhmeteff in 1911. It is merely the total energy per pound of fluid flowing in an open channel using the channel bottom as a datum plane. It can be expressed as:

$$\mathcal{E} = d + \frac{V^2}{2g} \tag{1}$$

Since $V = \frac{Q}{A}$, Equation (1) may be written in the form:

$$\mathcal{E} = d + \frac{Q^2}{2gA^2} \tag{2}$$

The depth for minimum specific energy can be found by differentiating Equation (2):

$$\frac{d\mathcal{E}}{d(d)} = 1 + \frac{d}{d(d)}\left(\frac{Q^2}{2gA^2}\right) = 0 \tag{3}$$

If the area of cross-section A can be expressed as a function of d the above derivation can be completed. For a rectangular channel $A = bd$, and Equation (3) becomes:

$$\frac{d\mathcal{E}}{d(d)} = 1 + \frac{d}{d(d)}\left(\frac{Q^2}{2gb^2d^2}\right) = 0$$

or

$$1 + \frac{Q^2}{2gb^2}(-2)\frac{1}{d_c^3} = 0$$

from which:

$$d_c = \sqrt[3]{Q^2/gb^2} = \frac{V_c^2}{g} \tag{4}$$

since $Q=Vbd$. Rearrangement of Equation (4) shows that critical velocity occurs when:

$$V_c = \sqrt{gd_c} \tag{5}$$

If the specific energy equation is divided by d_c or its equivalent values, as above developed, a dimensionless equation results[3]:

$$\frac{\mathcal{E}}{d_c} = \frac{d}{d_c} + \frac{1}{2}\left(\frac{d_c}{d}\right)^2, \tag{6}$$

a plot of which is shown in Fig. 1:

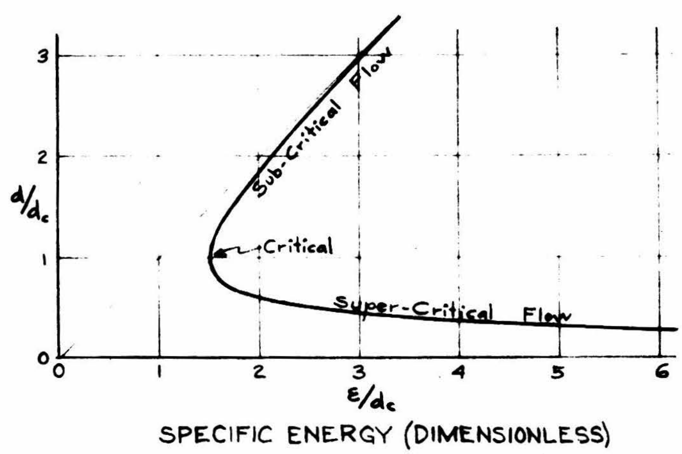

Fig. 1.

From this plot it can be seen that two entirely different conditions of flow are possible for a given specific energy, one with a large depth relative to the critical depth and the other small relative to the critical depth. The properties of flow on the upper portion of this curve are well known and have been utilized for many years. However, the properties of flow on the lower part of the curve, which are termed "super-critical", are not too well known.

With the studies that have been made in recent years on super-critical flow has come the realization that a definite relationship exists between the velocity of flow in a channel and the velocity of propagation of a gravity wave.

The velocity of propagation of an infinitesimal gravity wave, usually referred to as wave celerity, in still water, as first developed by La Grange, is given by the relationship:

$$C = \sqrt{gd} \tag{7}$$

It can be seen that the wave celerity increases with an increase in the depth of water. If a disturbance causing a wave occurs in a channel where there is already a velocity of flow, the one is superimposed upon the other, and the resulting velocity is the vector sum of the channel velocity and the wave velocity. The similarity of Equations (5) and (7) is at once apparent and examination shows that the two velocities are equal when $d = d_c$. Thus, if a disturbance occurs when the depth is critical; i.e., when specific energy is a minimum, the resulting vector velocity is zero and the wave thus created will be a stationary one so far as the upstream face is concerned.

When the conditions of flow in a channel are sub-critical; that is, when d is greater than d_c, and V is consequently less than V_c, it can be seen that the effects of a disturbance can be felt upstream from the source of the disturbance, since C will also be greater than V, and the wave created by the disturbance will travel upstream at a speed of $C-V$. However, when the flow conditions are super-critical, ($d < d_c$ and $V > V_c$), the effect of a disturbance cannot be transmitted upstream, since C will be less than V and the propagating wave consequently cannot travel upstream, but will be limited to a zone downstream from the disturbance. The limits of the zone can be determined readily by reference to the adjoining sketch, showing the vector velocities. The wave velocity C travels in all directions along the water surface at the same time it is being swept along downstream with a velocity V. The effects of any disturbance at "A" can only be felt within the boundaries of this zone. These boundaries are the sides of the angle 2β, where:

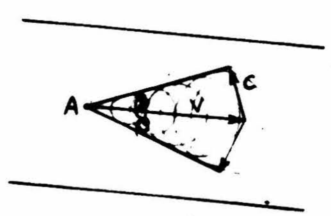

$$\beta = \sin^{-1}\frac{C}{V} = \sin^{-1}\frac{\sqrt{gd}}{V} = \sin^{-1}\frac{1}{F} \tag{8}$$

where F is the Froude number. β is known as the wave angle and is analogous to the Mach angle for super-sonic flow in gases[4].

B. REVIEW OF PREVIOUS STUDIES OF EFFECTS OF CURVES ON HIGH VELOCITY FLOW

The studies made by Knapp and Ippen, as previously cited[1,2], yielded results which gave for the first time clear concepts of the mechanism of super-critical flow in curves, with an understanding of the underlying reasons for the resulting disturbance patterns, both within the curves and downstream from them. Fig. 3 is a diagrammatic sketch showing the manner in which waves are built up in a curved section:

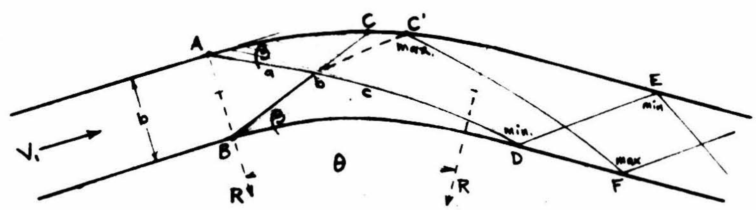

Fig. 3.

When the particles of water nearest the outside wall in the upstream straight section of the channel arrive at point A, the beginning of the curve, they are deflected by the curve through the angle β, whose magnitude is as shown by Equation (8). However, particles of water in the center of the channel continue in their original direction for a further distance downstream and are unaffected by the wall at the same cross-section, because of the inability of the wall to exert any influence on them. Particles near the inside wall are deflected at point B, the inside beginning of the curve, through the same angle β. As the particles a small distance from the outside wall in the upstream section pass through the infinitesimal wave created at point A and meet the curved section of the channel, they too are deflected and create additional waves, building up the wave front shown by points a, b, c. Also, as each particle further and further from the outside wall meets the curved wall, it builds up the depth of water along the wall. Downstream from point B, the wall is convex and the waves thus created are negative, with the consequent reduction in depth within the zone of influence of the disturbance at B. It would, therefore, be expected that the maximum depth along the outer wall would be attained when the effects of point B were first felt across the channel, point C. This is true except for a slight modification. Due to the increase of the wave velocity caused by the increased depth in the area AabC and the change in direction of the velocity in this area, the maximum depth is found downstream a small distance from C, or at point C'. Knapp and Ippen have shown that maximum depth occurs where:

$$\theta_0 = \tan^{-1} \frac{b}{\left(R + \frac{b}{2}\tan(\beta)\right)} \tag{9}$$

The depth of flow along the walls, at any angle θ below the beginning of the curve, which they calculated on the assumption of constant velocity throughout the curve (an assumption justifiable generally for super-critical flow because changes in depth are small compared to velocity-heads encountered) is given by:

$$d = \frac{V_1^2}{g} \sin^2\left(\beta \pm \frac{\theta}{2}\right) \qquad (10)$$

The plus and minum signs refer to outer and inner walls, respectively. The maximum depth is obtained by substituting Equation (9) in this latter expression and is found to be:

$$d_{max} = \frac{V_1^2}{g} \sin^2\left(\beta + \frac{\theta_o}{2}\right) \qquad (11)$$

It would be expected that these maxima and minima waves would be reflected back and forth across the channel in the downstream section, and so they are, gradually damping out with friction and other disturbances. The distance along either wall between two successive maxima, or between two successive minima, is:

$$L = \frac{2b}{\tan\beta} \qquad (12)$$

The first maximum depth as given by Equation (11) is greater than the other downstream maxima unless unfavorable conditions of reflection and interference are encountered further downstream.

C. ANALYTICAL APPROACH TO SUPER-CRITICAL FLOW AROUND A SHARP BEND

Even a hasty glance at the problem of attempting to analyze the mechanism of super-critical flow around a sharp bend indicates that it is essentially one involving three dimensions. Analysis of three-dimensional hydraulic phenomena is especially difficult. Since the present problem is concerned with reducing undesirable wall wave heights and the re-establishment of moderately uniform flow conditions in the downstream section, (both of which are essentially two-dimensional in scope), it is pertinent to make some simplifying assumptions which will allow a rational approach to the problem.

1. Assumptions:

The first assumption is that the distribution of pressure is hydrostatic. Actually pressure distribution is hydrostatic only if the curvature is gradual. However, Knapp and Ippens' studies of flow around curves indicated that the assumption of hydrostatic pressure distribution was permissible. Rouse[5], in an experimental study of high-velocity flow along a vertical plate at various angles to the original direction of flow, also determined that such an assumption was within satisfactory limits.

The second assumption is that of a velocity vector of constant magnitude, an assumption in close agreement with measured results.

2. Analysis of Wave Depths:

Fig. 4 indicates the wave which would be created by super-critical flow in a channel where the vertical outside wall changes abruptly in direction:

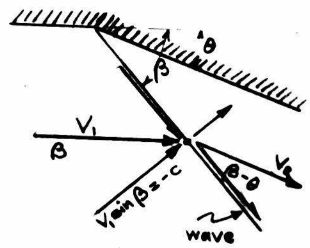

Fig. 4.

The velocity relationships are also indicated. At a point sufficiently removed from the wall to insure full development of the shock wave, application of the momentum and continuity principles should yield a relationship between the upstream and downstream depths.

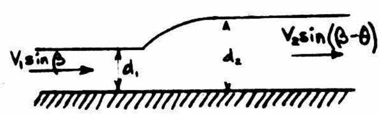

Fig. 5.

Fig. 5 indicates a cross-section through the wave front and normal to it. If the momentum equation is applied between vertical sections on each side of the wave front, there results:

$$\frac{W}{g} V_1 \sin\beta + w d_1 b \frac{d_1}{2} = \frac{W}{g} V_2 \sin(\beta-\theta) + w d_2 b \frac{d_2}{2} \quad . \quad (13)$$

Applying the continuity principle yields an additional necessary relationship:

$$W = wbd_1 V_1 \sin\beta = wbd_2 V_2 \sin(\beta-\theta) \quad , \quad (14)$$

use of the first part of which, substituted in Equation (13), results in:

$$\frac{1}{2}\left(d_2^2-d_1^2\right) = \frac{d_1V_1\sin\beta}{g}\left[V_1\sin\beta - V_2\sin(\beta-\theta)\right] \quad . \tag{15}$$

Also, from Equation (14):

$$V_2 = V_1\frac{d_1}{d_2}\frac{\sin\beta}{\sin(\beta-\theta)} \tag{16}$$

substitution of which in Equation (15), yields:

$$\frac{1}{2}\left(d_2^2-d_1^2\right) = \frac{d_1V_1\sin\beta}{g}\left[V_1\sin\beta - V_1\frac{d_1}{d_2}\sin\beta\right] \tag{17}$$

Equation (17) can be simplified to:

$$\frac{1}{2}\left(d_2^2-d_1^2\right) = \frac{d_1V_1^2\sin^2\beta}{g}\left(\frac{d_2-d_1}{d_2}\right) \tag{18}$$

which when solved for $V_1\sin\beta$ gives:

$$V_1\sin\beta = \sqrt{\frac{g}{2}\frac{d_2}{d_1}\left(d_2+d_1\right)} = C \tag{19}$$

This relationship, as pointed out by White and Rouse[6], is the same as that for a standing surge normal to the wave front.

Equation (19) can be rearranged into a more useful form:

$$\beta = \sin^{-1}\left[\frac{1}{V_1}\sqrt{\frac{g}{2}\frac{d_2}{d_1}\left(d_2+d_1\right)}\right] \tag{20}$$

and by recalling that $F = V_1/\sqrt{gd_1}$ can be simplified to:

$$\beta = \sin^{-1}\left[\frac{1}{F}\sqrt{\frac{d_2}{2d_1}\left(d_2+d_1\right)}\right] \tag{21}$$

It might be pertinent to point out that Equation (21) differs from Equation (8) by the term under the radical, - Equation (21) being that for a wave of finite height, while Equation (8) was that for an infinitesimal wave. One would expect, then, that Equation (21) should become Equation (8) when the conditions for an infinitesimal wave are applied to it. These conditions require d_2 to equal d_1, and this substitution is seen to satisfy the requirements.

By a few operations on Equation (21), it is possible to obtain a simple relation between d_2 and d_1. Thus:

$$2F^2\sin^2\beta = \frac{d_2}{d_1^2}(d_2+d_1) \tag{22}$$

Multiplying both sides by 4 and adding 1, gives:

$$1 + 8F^2\sin^2\beta = 1 + 4\frac{d_2}{d_1^2}(d_2+d_1) \tag{23}$$

which is equivalent to:

$$1+8F^2\sin^2\beta = \left(\frac{d_1+2d_2}{d_1}\right)^2 \tag{24}$$

Further,

$$\frac{d_1+2d_2}{d_1} - 1 = \sqrt{1+8F^2\sin^2\beta} - 1, \tag{25}$$

or

$$\frac{2d_2}{d_1} = \sqrt{1+8F^2\sin^2\beta} - 1 \tag{26}$$

Equation (26) then becomes:

$$\frac{d_2}{d_1} = \frac{1}{2}\left(\sqrt{1+8F^2\sin^2\beta} - 1\right), \tag{27}$$

a relationship giving d_2 for any value of d_1, provided β and F are known. Unfortunately, β is not usually known but must be determined in some other manner. In this regard, Equation (21) cannot be used because it is merely a rearrangement of Equation (27), and is, therefore, not an independent equation. However, an independent relationship can be obtained with ease. By reference to Fig. 4, it can be seen that the momentum equation applied parallel to the wave front will yield:

$$V_1 \cos\beta = V_2 \cos(\beta - \theta) \tag{28}$$

which, when applied as a divisor on Equation (14), gives:

$$d_1 \tan\beta = d_2 \tan(\beta - \theta) \tag{29}$$

This can then be rearranged to give the second relationship between d_2 and d_1:

$$\frac{d_2}{d_1} = \frac{\tan\beta}{\tan(\beta - \theta)} \tag{30}$$

If it is desired to separate β from θ, Equation (30) can be expanded readily to:

$$\frac{d_2}{d_1} = \frac{\tan\beta + \tan^2\beta \tan\theta}{\tan\beta - \tan\theta} \tag{31}$$

Equations (27) and (30) are thus two simultaneous equations, the solution of which gives β and the ratio d_2/d_1, θ being usually fixed in value, and F being constant depending on the value of d_1.

$$\begin{cases} \dfrac{d_2}{d_1} = \dfrac{1}{2}\left(\sqrt{1+8F^2\sin^2\beta} - 1\right) & (27) \\[2ex] \dfrac{d_2}{d_1} = \dfrac{\tan\beta}{\tan(\beta-\theta)} & (30) \end{cases}$$

Reference to Fig. 4 and the above development, would lead to the belief that the same analysis would apply in the case of a convex wall where a so-called negative shock wave would be encountered. Here, however, the values of θ would be ngative, or Equation (30) could be rewritten as:

$$\frac{d_2}{d_1} = \frac{\tan\beta}{\tan(\beta+\theta)} \qquad (32)$$

Little inspection of the two simultaneous equations is necessary to realize the difficulty of their solution. For that reason the accompanying chart, Fig. 6, has been prepared. For any value of θ and F, the corresponding values of d_2/d_1 and β can be determined quickly.

The area to the left of the line marked "Locus of minimum d_2/d_1" and above the line $d_2/d_1 = 1$ (or $\theta = 0°$) is the region to be used for the solution of the equations for positive shock waves, the only stipulation being that the flow at d_2 remain in the super-critical state.

The significance of the area above $d_2/d_1 = 1$, ($\theta = 0°$) and to the right of the line of minimum d_2/d_1 is believed to account for the flow conditions which would occur because of an obstruction or alteration changing the downstream flow from super-to sub-critical.

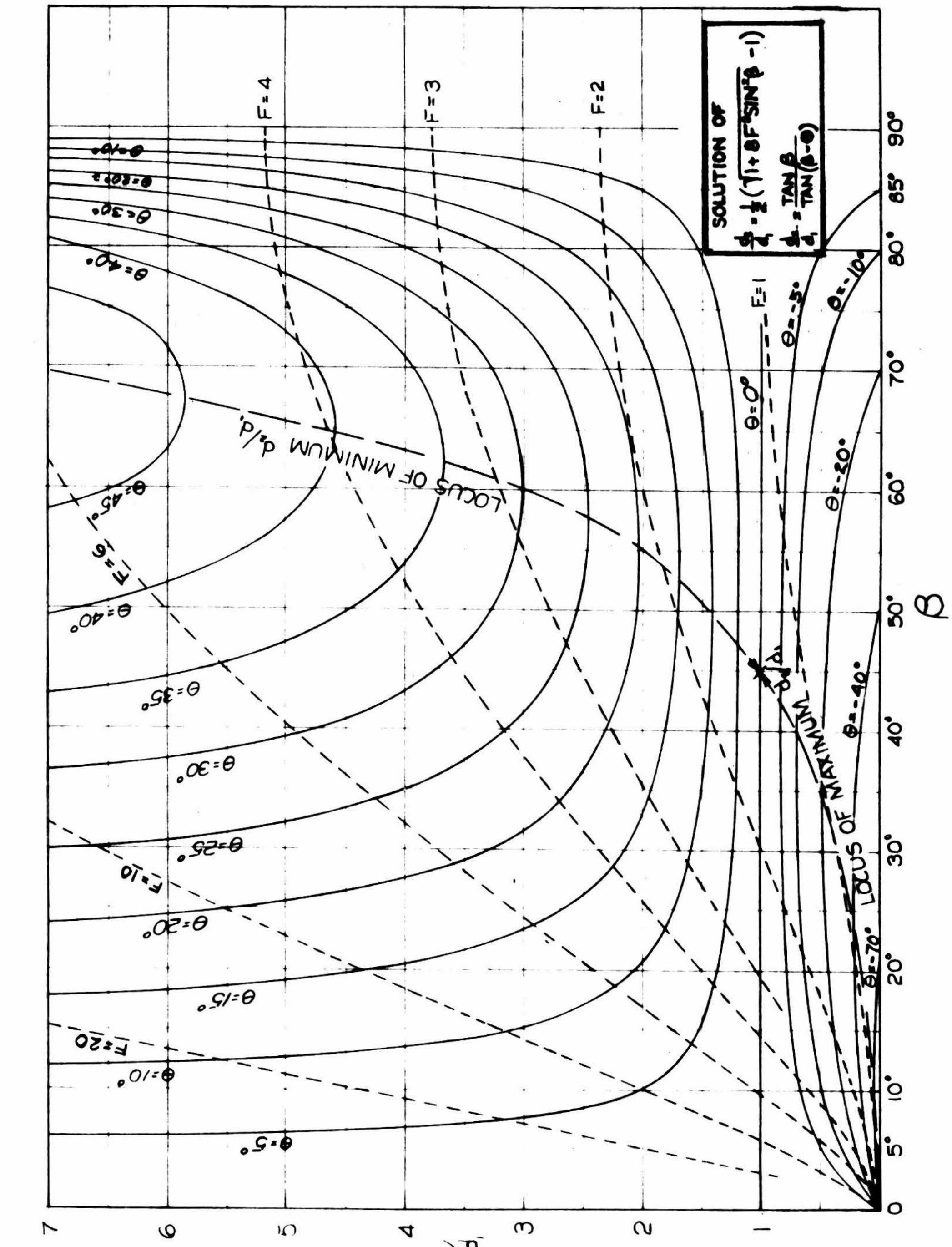
SOLUTION OF
LOCUS OF MINIMUM d2/d1
LOCUS OF MAXIMUM
F=1
F=2
F=3
F=4
F=6
F=10
F=20
θ=0°
θ=5°
θ=10°
θ=15°
θ=20°
θ=25°
θ=30°
θ=35°
θ=40°
θ=45°
θ=-5°
θ=-10°
θ=-20°
θ=-40°
θ=-70°
β
d2/d1

Fig. 6.

For example, with an angle of $\theta = 20°$ and $F = 4$, the depth ratio below the shock wave front would be 2.7 with a wave angle β of 34° if super-critical flow continues downstream. However, if sub-critical flow conditions existed downstream, or if the remedial measures applied within the channel bend caused the flow to change from super- to sub-critical, it is probable that a jump would occur and the downstream depth would then be 5.2 times the upstream depth and at an angle across the channel of $\beta = 85°$.

The region to the left of the line marked "Locus of maximum d_2/d_1" and below the line $d_2/d_1 = 1$ (or $\theta = 0°$) is that used for determining the downstream depth when so-called negative waves exist; as, for example, on the inside of a channel just below a bend. As an example, for a value of $\theta = -5°$ and $F = 3$, the ratio of d_2 to d_1 would be 0.75 and the wave angle β would be $15\frac{1}{2}°$.

No physical significance of the area below the $d_2/d_1 = 1$ line ($\theta = 0°$) and to the right of the maximum d_2/d_1 locus has been discovered by the writer at the present time.

3. <u>Location of Wave Crossings</u>:

While the downstream wave depths just determined apparently exist all along the shock waves, it is at once seen that near the boundaries the waves cannot be fully developed. On the outside wall the vertical acceleration produces a value of d_2/d_1 considerably in excess of that given by Equations (27) and (30), and on the inside wall the vertical deceleration produces a value of d_2/d_1 also larger than that given by the equations. It must also be remembered that "negative shock waves" are not physically possible, the wave actually being broadened out over a considerable distance.

The maximum depth along the outside wall could be expected to be located only a short distance below the change in direction of the channel. Unlike flow around a curve, no particular disturbance would be expected where the negative wave from the inside wall crossed to the outside wall. Below the negative wave front the water depth is decreased and this decrease should cause continued decrease in the water height along the outside wall below the point of reflection of the inside wave.

In Fig. 7, by the geometry of the figure the inside wall wave should reach the outside wall at:

$$R_{out} = b \tan \frac{\theta}{2} + \frac{b}{\tan(\beta + \theta)} \tag{33}$$

where β is the wave angle for the inside wall and could be determined by (a) Equation (21), (b) solution for β from Equation (31), or, preferably, (c) read from the chart of Fig. 6.

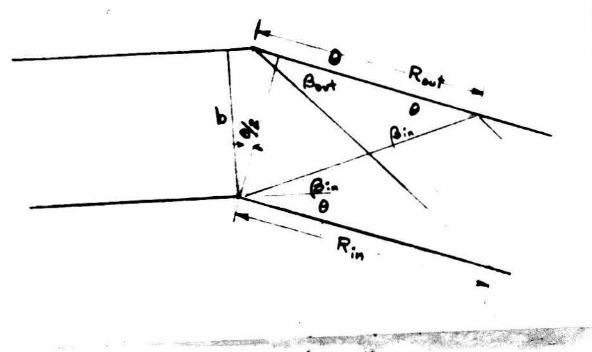

Fig. 7.

In a manner similar to the above, the point at which the shock wave created by the outer wall reaches the inside wall should be at a distance R_{in} where from Fig. 7:

$$R_{in} = \frac{b}{\tan(\beta-\theta)} - b\tan\frac{\theta}{2} \qquad (34)$$

In this equation β is the wave angle for the outside wall. The disturbance created along the wall at this point could be expected to be rather severe in view of the fact that this is the positive wave front. Undoubtedly, the water will attain considerable height here.

Immediately upstream from the wave front, because of the negative wave effects, a very small depth of water should be encountered.

The wave reaching point R_{in} could now be expected to be reflected diagonally back to the outside wall of the channel reaching it at a point approximately equal to 2 R_{in}. It would thereafter cross back and forth across the channel as it progressed downstream, hitting consecutive points along the channel with the wave length:

$$L \approx 2 R_{in} \qquad (35)$$

It is important to point out that although the two wave angles β mentioned above might at first appear to be the same in magnitude, reference to the chart of Fig. 6 will show that β for the outside wall will not be the same as β for the inside wall.

D. ANTICIPATED EFFECT OF SILLS ON WAVE REPRESSION

1. Wall Wave Heights:

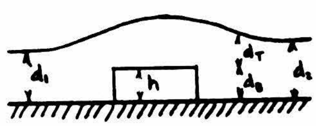

Fig. 8.

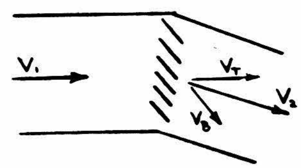

Fig. 9.

Echelon placement of submerged sills, as shown in Fig. 8 and Fig. 9, would be expected to divide the flow of water into two layers, a bottom layer whose flow direction would be parallel or approximately parallel to the sills, and a top layer, whose flow direction would depend upon the principles developed in the preceding sections. If the angle of the sills to the upstream channel walls is α, the bottom layer would be deflected at approximately the same angle throughout the width of the channel. The top layer would continue on, with a rise due to the bottom pressure influence but with little direction influence from the sills, until affected by the inside and outside changes in wall direction. If the angle α were greater than θ, a piling up of the water on the inside of the channel and a reduction of the quantity of water along the outside of the channel could be expected as a result of the turning of the bottom layer. Superimposed on this would be the negative wave on the inside portion of the channel, tending to reduce the depth of flow and a shock wave on the outside tending to increase the depth of flow. By proper sill selection, arrangement, and angle of attack, it should, therefore, be possible to reduce drastically or repress the undesirable depths of flow along the outside wall below the bend and at the same time increase the low depths of water along the inside wall. The ideal wall profiles would be those of uniform flow. While it would be desirable to reduce wave heights within the central portions of the channel, these are not nearly so important as the reduction or suppression of the water heights along the walls.

2. Reduction of Transverse Velocity:

In addition to reducing the outside wall water heights and increasing those along the inside wall, any sills to be satisfactory must be capable of sufficient reduction of the overall transverse velocities as to assure positive non-recurrence of objectionable waves anywhere downstream from the bend.

There is a certain amount of energy loss within the wave itself. By substitution of the shock wave velocity:

$$C = -V = \sqrt{gd_1}\left[\frac{1}{2}\frac{d_2}{d_1}\left(\frac{d_2}{d_1}+1\right)\right]^{1/2} \tag{36}$$

(which is the same equation as (19) without the sin β factor, as previously mentioned), into the specific energy relationship:

$$\Delta\mathcal{E} = \mathcal{E}_1 - \mathcal{E}_2 = d_1 + \frac{V_1^2}{2g} - d_2 - \frac{V_2^2}{2g} \tag{37}$$

Rouse[7] determined the loss due to turbulence at the wave front to be:

$$\Delta\mathcal{E} = \frac{(d_2-d_1)^3}{4d_1d_2} \tag{38}$$

Fig. 10 shows a channel with an abrupt bend in which are placed a series of sills, echelon fashion, at an angle α with the upstream walls. The forces which are absorbed by the sills due to the dynamic action of the water impinging upon them, are represented by P_x and P_y, being parallel to and normal to the original direction of flow, respectively. ϕ in this figure represents the effective angle of turn of the water as a whole, due to the effects of the sills.

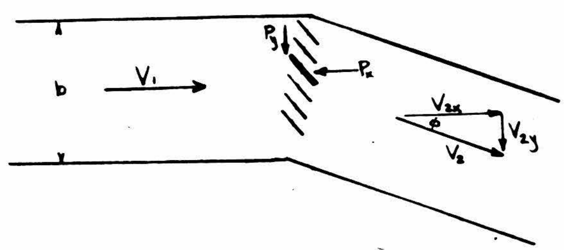

Fig. 10.

Application of the continuity principle to the upstream and downstream sections, assuming that the velocity distribution is uniform throughout each section, gives:

$$W = wbd_1V_1 = wbd_2V_2 \tag{42}$$

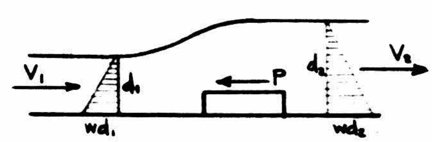

Fig. 11.

Since force can be represented as the time rate of change of momentum, the force exerted by the sills can be included in the following equation, indicating the transport of momentum in the x-direction:

$$\frac{W}{g}V_1 + wd_1\frac{d_1}{2}b = P_x + \frac{W}{g}V_{2x} + wd_2\frac{d_2}{2}b \qquad (43)$$

Substitution of Equation (42) yields:

$$\frac{wd_1bV_1}{g}V_1 + \frac{wbd_1^2}{2} = P_x + \frac{wd_1bV_1}{g}V_{2x} + \frac{wbd_2^2}{2} \qquad (44)$$

or

$$V_1 + \frac{gd_1}{2V_1} = P_x\left(\frac{g}{wbd_1V_1}\right) + V_{2x} + \frac{gd_2^2}{2d_1V_1} \qquad (45)$$

If the total force in the x-direction divided by the mass of water flowing per second is defined as J_x ; i.e.:

$$J_x = P_x \div \frac{W}{g}$$

Equation (45) can be rewritten in the form:

$$V_1 + \frac{gd_1}{2V_1} = J_x + V_{2x} + \frac{gd_1V_1}{2V_{2x}^2} \qquad (46)$$

where J_x has the dimension of a velocity. Next, consider $V_{2x}=V_1-u$ where u is, for the moment, the decrease in velocity in the x-direction due to the effect of the sills. Substituting this in (46), gives:

$$V_1 + \frac{gd_1}{2V_1} = J_x + V_1 - u + \frac{d_1V_1g}{2(V_1^2-2V_1u+u^2)} \qquad (47)$$

or

$$\frac{gd_1}{2V_1} = J_x - u + \frac{d_1g}{2V_1}\left(\frac{1}{1-2\frac{u}{V_1}+\frac{u^2}{V_1^2}}\right) \qquad (48)$$

Because the angle of turn is relatively small, no appreciable error will be introduced by dropping the term u^2/V_1^2 and expanding the last term by the binomial theorem:

$$\frac{gd_1}{2V_1} = J_x - u + \frac{d_1 g}{2V_1}\left(1 + 2\frac{u}{V_1} + \cdots\right) \tag{49}$$

This reduces to:

$$J_x = u - \frac{d_1 g u}{V_1^2} = u\left(1 - \frac{1}{F^2}\right) \tag{50}$$

from which

$$u = \frac{J_x}{\left(1 - \frac{1}{F^2}\right)} \tag{51}$$

substitution of which back into the relationship defining u gives:

$$V_{2x} = V_1 - u = V_1 - \frac{J_x}{\left(1 - \frac{1}{F^2}\right)} \tag{52}$$

In the y-direction of Fig. 10:

$$P_y = \frac{W}{g} V_{2y} \tag{53}$$

If now J_y is defined as $P_y \div \frac{W}{g}$, the above becomes:

$$J_y = V_{2y} \tag{54}$$

Hence, the effective angle of turn ϕ is such that:

$$\tan\phi = \frac{V_{2y}}{V_{2x}} = \frac{J_y}{V_1 - \frac{J_x}{\left(1 - \frac{1}{F^2}\right)}} \tag{55}$$

or, reconverting J_x and J_y :

$$\phi = \tan^{-1} \frac{\frac{P_y \cdot g}{wbd_1V_1}}{V_1 - \frac{\frac{P_x \cdot g}{wbd_1V_1}}{\left(1 - \frac{1}{F^2}\right)}} \tag{56}$$

And, finally:

$$\phi = \tan^{-1}\left(\frac{P_y}{wbd_1^2F^2 - \dfrac{P_x}{\left(1-\frac{1}{F^2}\right)}}\right) \tag{57}$$

The term $wbd_1^2F^2$ is recognized as the upstream momentum factor. Thus, Equation (57) tells us that the effective angle through which the water in the channel is turned is that whose tangent is the ratio of the pressure exerted on the sills at right angles with the original direction of flow to the difference between the original momentum and the pressure exerted on the sills in the direction of flow, (corrected by a factor to account for the relative velocities of wave celerity and the channel velocity).

III. EXPERIMENTAL STUDY

A. APPARATUS AND EQUIPMENT

1. Preliminary Studies:

Considerable preliminary studies were made on two trial channels before comprehensive detailed experimentation was started. One channel was constructed of galvanized iron and had a bottom width of 12 inches and a depth of 9 inches. A 15° sharp bend was built into its approximate midpoint, with an approach and downstream section each approximately 25 feet long. Serious difficulties were

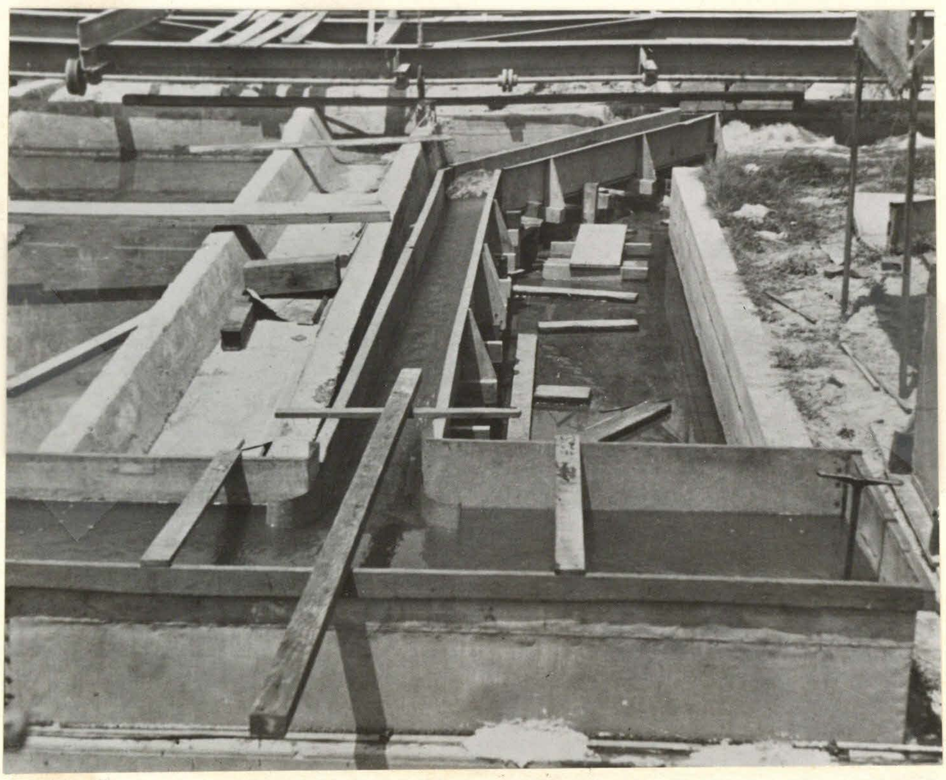

Fig. 12.

encountered in establishing uniform flow in the short distance before the bend, but these were finally overcome by adding a specially designed entrance section. Bottom stability was difficult to obtain until the channel bottom was heavily braced to prevent deflections in the channel material. Fig. 12 is an over-all view of this channel.

Fig. 13.

Fig. 13 is a view showing the piling up of the water and the cross-actions of the waves created by the bend in the channel.

The studies made in this channel, the knowledge gained in its construction, and the determination of its unsatisfactory features, led to the belief that a wider channel of heavier material with closer control of the quantity of water flowing would be desirable. A smaller degree of bend was also deemed essential in order to study properly the effects of the sharp bend and the possible corrective treatments to be applied.

2. The Channel:

A brass channel, belonging to the Hydraulic Structures Laboratory of the Institute, was made available for the continuance of this work, through the kindness of Drs. Knapp and Vanoni.

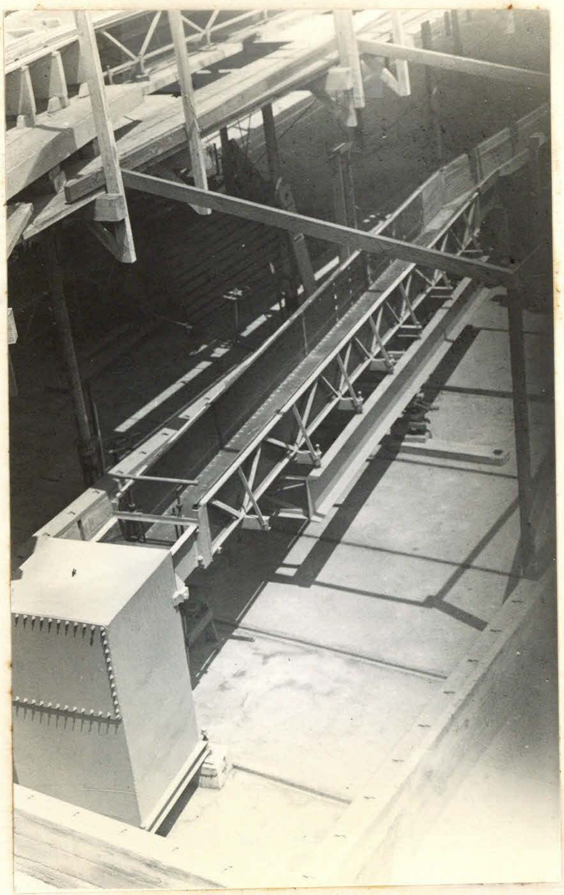

Fig. 14.

This new channel was 18 inches wide, 12 inches deep, and 30 feet long. It was equipped with an entrance box and a completely independent water system, including remote control operation of the pumping unit. A 10° bend was constructed in the channel at a point approximately 20 feet from the entrance section, allowing a 10 foot downstream section. Many runs were made in this channel on a slope of 0.0431. Due to the short section below the bend, a full downstream picture of flow conditions could not be obtained, and to this downstream section was then added a 10 foot section of heavy galvanized iron to allow the waves created in the bend to cross and recross the channel before the water spilled out over the lower end. Fig. 14 and Fig. 15 give a general view of the channel and its appurtenant equipment. Drawings A, B, and C indicate the details of construction, wiring, etc. It was originally intended that the slope of the channel be adjustable, but such did not prove practicable, because of the necessity of redesigning the bend for each change of

Fig. 15.

slope and the difficulties encountered in moving the entire channel as a body to prevent wall buckling.

Fig. 16 shows the layout for the 10° bend as actually constructed and built into the channel. It is pertinent to point out that in order to maintain a level bottom in the channel normal to the direction of flow, a modification of this design would have been required for each particular slope.

The slope of the channel was carefully adjusted to obtain a five per cent slope longitudinally along the channel and level conditions across the channel at each cross-section.

The entire channel was equipped with a substantial and well graded track on either side which served as a support means for measuring depths, velocity magnitudes, and velocity directions. The channel measurements

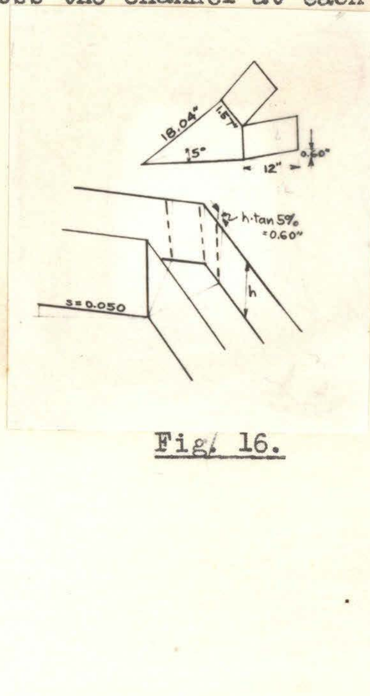

Fig. 16.

were made with the inside wall of the bend as a zero point, termed in all the data as CB. Upstream stations were marked with the prefix "U", while downstream stations were marked with the prefix "D". The outside wall of the channel at the center of the bend was also marked CB, but station U-0 was directly across the channel from the inside center of the bend with relation to the upstream portion of the channel, and D-0 was directly across the channel from the inside center of the bend with respect to the downstream end of the channel. A paper scale, varnished, was placed on the track and served at all times to insure exact longitudinal station location with a minimum of error.

3. Entrance Section of Channel:

The entrance section provided a ready means of establishing uniform flow conditions in the upstream section of the channel. It consisted of an adjustable gate with scales and verniers attached for the purpose of obtaining equal water depths throughout the entrance control section. Fig. 17 is a close-up view of the entrance section. A view of the entire entrance box can be seen in Fig. 14.

Fig. 17.

Fig. 18.

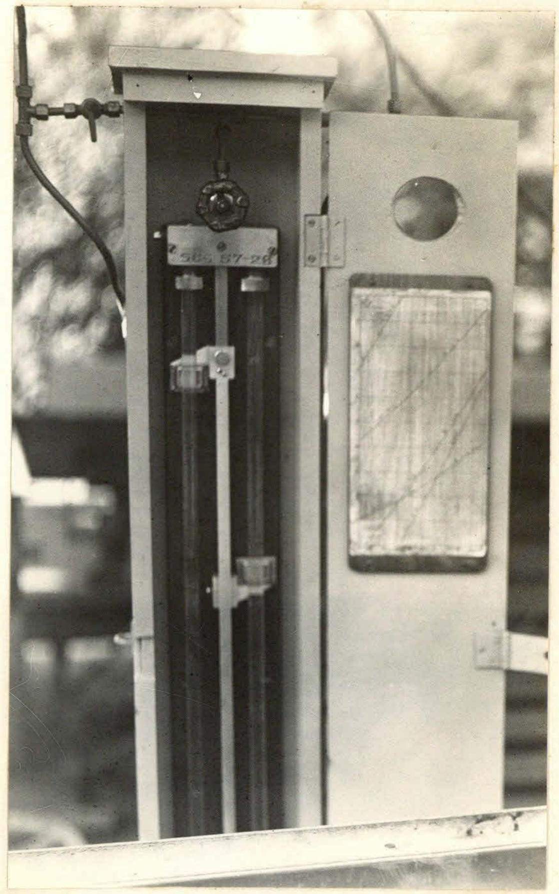

Fig. 19.

4. Source of Water and the Circulating System:

Water for the operation was stored in a sump below the surrounding ground level beyond the downstream end of the channel. The circulating pump was driven by an electric motor, the two being interconnected with a variable speed friction pulley, V-belt driven. The impeller of the pump was set below the water level in the sump so as to be primed at all times. Water was pumped from the sump to a 12 inch horizontal pipe which ran the entire length of the channel and discharged into the entrance box. The quantity of flow was determined by a well-calibrated Venturi meter. Fig. 18 is a closeup view of this Venturi. The pressure lines from the Venturi were run directly overhead to a water manometer, which was housed in a weather-proof box and contained, as well as the manometer, a carefully plotted diagram showing the discharge for any differential head reading of the manometer. Provision was made for bleeding all manometer lines at the start of operations. Fig. 19 is a view of the manometer with its housing and calibration curve.

To summarize then, the circulation of the water was as follows: From the sump the water was pumped into the horizontal pipe running the length of the channel. Near its midpoint, a Venturi meter was inserted which allowed accurate determination of the quantity of flow at any time. The water from the 12 inch pipe discharged into the entrance box. With proper adjustment of the entrance box, uniform flow could be maintained with only insignificant variations. The water flowing out of the channel at its lower end discharged into a large basin where it was circulated by the pump back into the pipe to repeat its previous process. The discharge could be maintained at a very constant value by means

Fig. 20.

of remote control of the pump speed. This remote control permitted experimental runs of fairly long duration to be made at any specific value of discharge, thus maintaining consistent conditions of flow over long periods of time. Fig. 20 is a view of the end basin, the pump house, and the trench which contained the 12 inch circulating pipe.

B. INSTRUMENTS

1. Point Gage:

The depth of flow at any point was determined readily by the use of a point gage which was especially built for the channel. As seen in Fig. 21, it consisted of two brass angles spaced 4 inches apart and mounted on a single plate at one end and a 12 inch length of channel iron at the other end. The channel iron contained a grooved roller at each extremity which ran on the track previously described. The plate slid on the track on the opposite side of the channel. Mounted on the supporting plates was a heavy scale which held the point gage. An integral part of the point gage was a vernier which permitted the reading of depths to .001 feet. The point gage could be readily moved up and down, and with a friction spring which was built into the bottom supporting base was held in any vertical position with ease. The upstream cross angle iron was also scaled so that setting of the point gage across the channel could be made readily and accurately.

Fig. 21.

2. Pitot Tube:

A pitot tube, made of a hypodermic needle, served as the means of determining velocities at any point in the channel. Because of the minute size of the needle, it was possible to determine velocity magnitudes at almost any point desired, including velocities within 0.02 feet of the walls or 0.002 feet of the bottom of the channel. The hypodermic needle was attached to a brass tube which served as a means of support and also as an inter-connecting link between the needle and a glass tube used for measuring the velocity heads. The glass tube was of a sufficient length to permit measurement of the maximum velocities that were encountered. A scale was glued to the vertical support which held the glass tube, and the whole assembly was clamped to the point gage in such a manner as to allow free vertical movement up and down with the point gage and horizontally across the channel. The needle could be turned in any direction desired so that velocities not only in the direction of flow were

Fig. 22.

measured, but transverse velocities could be obtained as well. The pitot tube point, its mounting and inter-connecting linkage with the glass tube, can be seen in the left-hand side of Fig. 22.

3. Velocity Direction Gage:

Fig. 22 also shows the velocity direction gage, which was developed and built by the author at the suggestion of Dr. Knapp, to determine the velocity direction at any point in the channel. The velocity direction gage was also built into the point gage support in somewhat the same manner as the pitot tube and served as an integral part of that instrument. Hence, velocity directions could be determined at any point and with but a slight shift of the instrument the corresponding magnitude could be determined at the same point. The velocity direction gage consisted of a 1/16 inch vertical rod with a vane at its lower and upper ends. The rod was inserted within a suitable mounting to allow ease of rotation and to give sufficient support and rigidity against bending which might occur as a result of the high velocities involved. The upper vane was soldered to the rotating shaft after insertion in the supporting member. The position of the lower vane thus was transmitted directly to the upper vane. Immediately below the upper vane was placed a finely graduated circular scale for determination of the velocity direction. The upper vane was carefully correlated with the lower vane and checked at the beginning and end of each day's experimentation. Direction angles could be read to within one-half degree, under normal conditions. Movement vertically was provided in the same manner as that for the point gage.

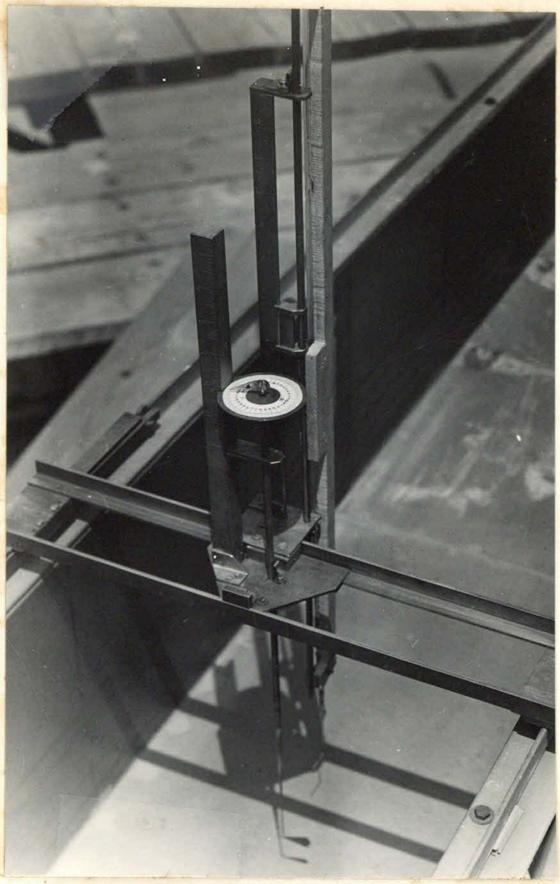

Fig. 23.

This apparatus, with its direction gage, is illustrated in Fig. 23. The friction spring which served to hold the gage at any elevation in the channel can easily be seen. Fig. 24 is a general view of the combined pitot tube and velocity direction gage.

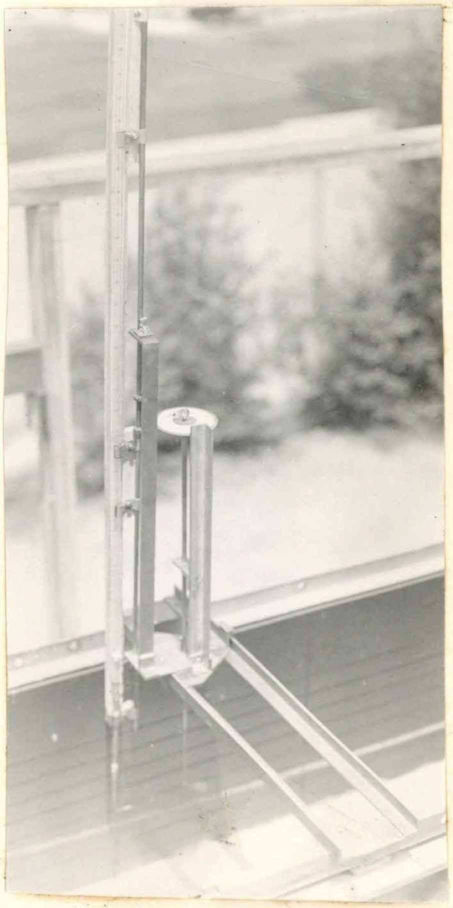

Fig. 24.

4. Sills:

Preliminary investigations over a period of several weeks disclosed that one or two single long sills stretching diagonally across the bottom of the channel were not a suitable corrective device for reducing the undesirable waves created by the bend. It may be pointed out that in a

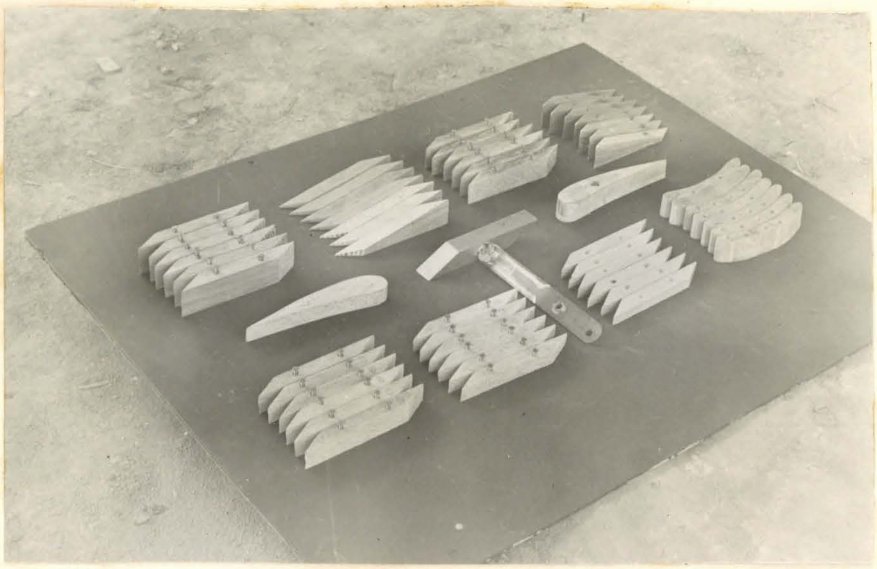

Fig. 25.

long radius bend in a rectangular channel two or three strategically located sills extending across the channel serve as a fairly suitable remedy. These preliminary investigations, coupled with an attempted mathematical analysis of the problem, led to the belief that a single sill cut up into short lengths and placed in parallel across the channel would accomplish the purpose desired. Fig. 25 is a view of a small part of the many different types of sills used in this study. The sill in the center of the picture was made of brass and welded to a heavy steel shank sharpened to a knife edge on both edges to permit studies of the effects of a single sill at any point in the channel. Fig. 26 is a view of a typical set of sills mounted in place in the channel. The sills were fastened to the channel bottom by brass bolts running the full depth of the sill and tapped into

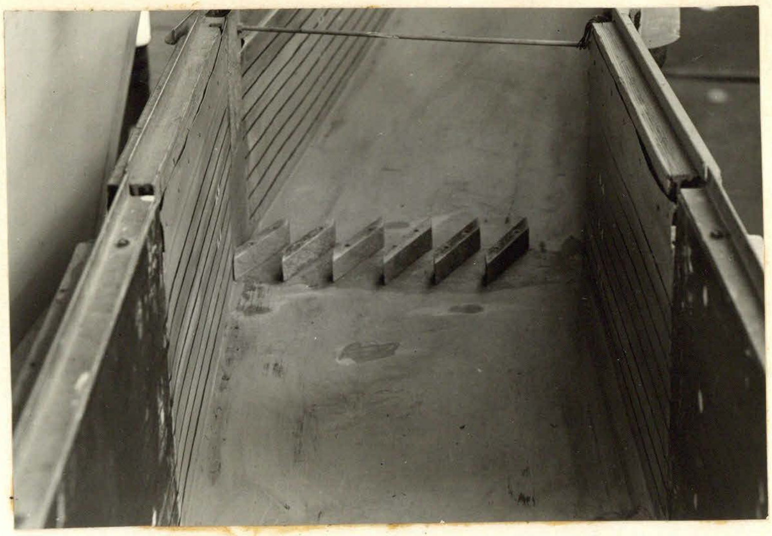

Fig. 26.

the channel. This method of mounting also gave stability to the sills and enabled them to withstand the relatively high dynamic forces exerted against them by the flow at the high velocities used in this research.

5. Scales:

A very ingenious method of measuring the forces acting on the sills was suggested by Dr. Merit P. White and, with minor improvements and variations is shown in Fig. 27. The sills were mounted on a thin sill plate, as shown in Fig. 28. The upstream edge of the sill plate was allowed to move freely longitudinally and laterally, but was prevented from moving vertically any appreciable amount by small clearance washers, as shown between sills 2d and 3d and between sills 4d and 5d in the figure. Two lines were attached to the upstream edge of the sill plate, one to the downstream edge and one to

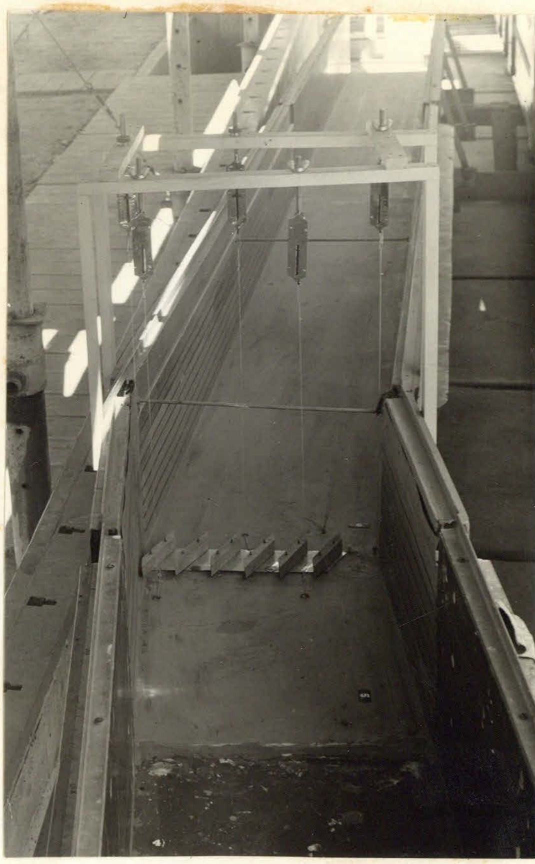

Fig. 27.

either end of the sill plate. Each line ran horizontally from the sill plate sufficiently far to eliminate any appreciable effects of the minute pulleys and their supports which served to transmit the force from a horizontal direction to a vertical direction, and thus permit measurement of the forces on scales. Regulation of the position of the sill plate was made by adjusting nuts on the support rod of the scale. The bolts which held the sills to the sill plate did not extend through the sill plate, but were merely mounted upright upon it with the heads soldered to the plate.

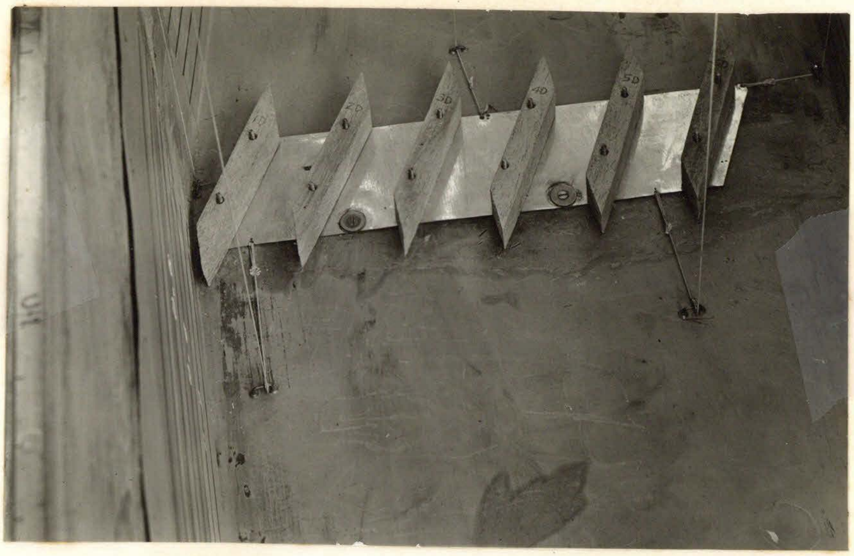

Fig. 28.

C. EXPERIMENTAL PROCEDURE

1. Adjustment of Flow:

The experimental apparatus including the channel, pumping system, and all instruments to be used, were given a quick inspection daily before each run to insure validity of the basic data. At periodic intervals the channel slope was also checked, but at no time was any variation discovered.

While some minor difficulties were encountered during the early stages of the experimentation, they soon led to a standard method of starting the equipment for each day's run. The method adopted was first to open slightly the valve on the discharge side of the pump. The pump was then started and by the remote control was slowed down or speeded up to the point where the discharge through the system was approximately 1 cu.ft. per sec. The manometer lines were bled of unwanted air and the entrance box was adjusted to the proper opening to correspond with the uniform depth of flow for the discharge desired. Provision was made in the entrance box for bleeding all air from the box at its highest point, and once or twice during each experimental run any air collected in the entrance box was let out through the bleed valve.

Once all the air was removed from the entrance box and uniform flow conditions obtained, the pump speed was adjusted by remote control at a point near the manometer box to bring the quantity of water flowing up to the desired amount. The remote control permitted adjustment of the flow over an extremely narrow range so that all runs were made at practically a constant discharge. Water passing through the channel and on into the tailrace passed through a fine screen and on into an intermediate sump from which it was again picked up by the pump and circulated back through the system over and over again for as long a period of time as was necessary for the run.

The value of "n" for use in the Manning formula had been extensively determined from experiments by Knapp and Ippen in a similar channel and also by Rouse in the same channel. It was felt unnecessary to analyze the channel further for its roughness coefficient, in view of the compatible results of these experimenters.

2. Profile Measurements:

All studies made in the channel, with a few exceptions at the beginning of the experimentation, were those for a constant discharge and steady uniform flow conditions in the upstream section of the channel. Once such flow was established for the desired discharge, profile measurements were made from section to section downstream from the bend by use of the point gage, and also at three or four stations upstream from the bend to assure absolute check on the uniform flow assumption. The point gage described under "Experimental Apparatus" provided a quick means of reading depths of water at any point within the channel. The depth of the water surface was first read and recorded in a book suitable for that purpose, and entered immediately below that figure was the depth of the bottom of the channel. Early experimentation was carried on for profile measurements by recording the bottom profiles for the entire channel on a single page of the data book and it was thought that reading and recording of the water surface heights would be the quickest means of determining the complete profile. It took but little experimentation to learn that it was far simpler to set and read the point gage for the water surface and the channel bottom at the same point than to compute the depth of water as a separate step. Complete profile measurements were taken for the untreated channel flow at discharges of 1.0, 2.0, 3.0, and 4.0 cu.ft. per sec. Particular attention was paid to the outside and inside wall profiles in order to have an accurate plot of such profiles throughout the available length of channel. Sill selection was based primarily on the results obtained from wall profile measurements with the many and varied types of sills in place in the channel angle.

3. Velocity Measurements:

The velocity direction gage and pitot tube were carefully calibrated to determine any unanticipated characteristics which they might contain. Fortunately, no eccentric characteristics were found. Readings of velocity magnitude and direction were made by placing the bottom vane of the velocity direction gage at the point where the velocity was to be measured and reading the angle indicated on the circular scale by the upper vane. Careful attention was paid to the location of the point involved and the pitot tube then was moved to the same point. The direction of the velocity having been determined as just described, the pitot tube was pointed in the same direction and the height to which the water rose in the glass section of the pitot tube was read and recorded. The pitot tube was so mounted that it could be turned with ease in any desired direction.

This method of measurement was sufficiently accurate to allow the determination of the velocity at any point in the channel above 0.002 feet from the bottom of the channel, and to within 0.02 feet of either wall. Velocity measurements required considerable time at each station and for that reason comprehensive studies were made only for the maximum discharge with untreated flow and later with the best treatment obtained.

4. Sill Selection:

Careful analysis of the many and varied experiments conducted by Knapp and Ippen in long radius curves in a rectangular open channel, led to the belief that a single sill extending diagonally across the channel could not be a satisfactory means of repressing the waves created in a bend. As previously mentioned, brief experimentation indicated that great possibilities could be obtained by cutting the single long diagonal sill into short lengths and placing them echelon fashion approximately at the bend. All types of sills were tried, ranging in shape from wide, triangular-shaped sections to narrow, vertical walls confining the flow within narrow limits.

Many difficulties were encountered and the results obtained by nearly all the types of sills tried were very discouraging. One of the principal requirements was that the sills should be self-cleaning and under no conditions induce the piling up of any debris that might be present in a full-scale channel. It was soon learned that the sill on the extreme inside wall would have to be removed. It exerted such a drastic diversion effect as to cause an excessive and prohibitive piling up of water on the inside channel wall. Many sills performed favorably under the largest discharges experimented with, yet under low discharges they were entirely unsuitable. An example of this can best be illustrated by reference to Fig. 29, which shows the disturbance caused by an otherwise satisfactory set of sills. Another serious difficulty encountered with many of the sills used was separation of the water in flowing around the back of the sill. This separation produced air pockets which entrained air in the water, the entrained air passing on downstream. At the same time the air pockets evidently bordered on the edges of what was believed to be cavitation. The rapid intermittent collapse and reformation of the air bubbles frequently made very loud explosive-

Fig. 29.

type noises, and loosened the bolts holding the sills to the channel bottom. No other effects, however, were apparent on the sills themselves. In an effort to overcome this defect, airfoil-type sills were installed, but as would be expected, the water in its supercrtical state would not follow the sill contour. Of all the sills experimented with, only two sets or arrangements were deemed sufficiently satisfactory to be worthy of extensive study, and complete velocity measurements and profile measurements were made with these sills in place. In all other cases, the maximum and minimum downstream disturbances only were recorded and remarks made as to the separation features and the ability to self-clean.

The large sill discussed in the section under "Instruments" and pictured in the center of Fig. 25, aided greatly in determining the direction at which the sills should be placed, their location within the channel, and their relative nearness to one another.

5. Measurement of Forces Acting on Sills:

The components of the total force acting on a particular set of sills were measured by means of a sill plate, as previously discussed, through which force components were transmitted to scales above the channel. Sufficient disturbance was made on the sill plate before each reading to insure complete freedom of movement of the sill plate. All scales were adjusted to an arbitrary pre-determined zero, with the sills in place but with no water flowing. The water was then allowed to attain equilibrium conditions and the scales readjusted so that a direct reading of the force acting could be made. Little experimentation was needed to satisfy the condition of free movement of the sill plate, because readings of the forces for the same flow conditions following disruptions always showed a set consistency.

6. Photography:

It was found desirable at the outset, due to the length of each run, to record by pictures as much of the flow conditions as could satisfactorily be so obtained. Pictures of the flow conditions were difficult to get, because of the rapid movement of the water; the poor lighting available because of the channel being located below a large platform; and because of the direction at which pictures had to be taken. A vertical picture of the flow phenomena was impossible over sufficient range to be of suitable use. Neither could such a picture indicate with any degree of discernment the relative water surface contours and profiles. It was, therefore, necessary to take all pictures either facing the downstream or the upstream sections. Several hundred photographs were taken but only a small number is included in this thesis.

D. EXPERIMENTAL RESULTS

The experimental results obtained are presented both graphically and by photograph wherever possible. In many instances a photographic view is not at all feasible, as, for example, in the case of velocity distribution within a cross-section. Other results are presented only in photographic form, an actual picture conveying many times more than could be displayed in graphic form.

1. Sill Selection:

As previously discussed, many and varied were the types of sills used in this research. The series of sills experimented with in the preliminary work were denoted by number, such notation being entirely satisfactory so long as all sills in a set were of the same shape and size. But, with the addition of the ten foot length to the downstream end of the channel, a new system of designating each sill had to be devised. Each set of sills was arbitrarily assigned a letter denoting the series or grouping and each individual sill was assigned a number to indicate its position with respect to the outside wall, the sill nearest the wall carrying the number "1", etc. The sills shown in Fig. 25 are grouped in such a manner that all sills of the same size and shape are together. In the early experimentation each group was used as a whole; i.e., all sills in any group were equivalent in shape and size. Such a set of sills can be seen in Fig. 26, where the "B" sills are shown in place in the channel. Each sill is the same as every other sill.

The advantages of using various sizes of sills in a series were discovered with the addition of the downstream length of the channel. While it was obviously impracticable to attempt to investigate the characteristics of all the various possible combinations of sills, this was not necessary because certain combinations immediately eliminated themselves and similar ones when tested. The best combination which the writer was able to discover was known as the K series, pictured in Fig. 30. All sills in this series were 3/4 inches wide and 5 inches long, but varied in height. The sill nearest the wall was 1 inch high, sills Nos. 2, 5, and 6 were 1-1/4 inches high, and Nos. 3 and 4 were $1\frac{1}{2}$ inches high.

Fig. 30.

Another series, known as the I-series, performed much better at the high discharges and velocities, but were unsuitable at low values of discharge and velocity. Table I. contains a summary of the seven best series of sills tested, along with four series of equal size sills, and conditions of untreated flow for comparative purposes. The figures comprising the body of the table indicate inside or outside maximum wall depths for a discharge of 4.0 cu.ft. per sec.

TABLE I
COMPARISON OF MAXIMUM WALL DEPTHS vs. SILL TYPES

SILL SERIES	MAXIMUM WALL DEPTHS * AT D-2	NEAR D-4	NEAR D-10.5	NEAR D-18	SILL HEIGHTS IN INCHES ‡ #1	#2	#3	#4	#5	#6
none	478	487	565	577	no sills					
D	214	415	372	452	all 3/4 inches					
C	271	387	343	420	all 1 inch					
B	331	379	335	405	all 1¼ inches					
A	378	342	304	394	all 1½ inches					
K	331	352	341	346	1	1¼	1½	1½	1¼	1¼
I	306	361	320	345	1	1¼	1½	1¼	1	1¼
F	286	368	341	348	1	1¼	1½	1¼	1	1
H	290	374	370	356	1	1½	1½	1½	1	1
E	349	344	355	369	1¼	1¼	1½	1½	1¼	1¼
J	326	366	314	369	1	1¼	1½	1¼	1¼	1¼
L	306	375	372	371	1	1¼	1½	1½	1¼	1

*All depths are in thousandths of a foot. ‡All sills are 3/4" wide by 5" long.

Depths under the column headed Station D-2 are depths at that station. Stations D-4, D-10.5, D-18 merely denote the approximate location of the maxima, the maxima shifting slightly one way or the other depending on the sill series used. The maxima, of course, occur first on the outside wall, then on the inside wall, and again on the outside wall, literally bouncing from one wall to the other, as indicated by the untreated flow pattern (Q = 4.0 cu.ft. per sec.) in Fig. 31.

It might be pointed out in Table I. that the effects of an increase in height of similar sills (series D, C, B, A) are to reduce any given maximum, although the reduction is not a uniform one between different maxima. At Station D-2 a small sill height decreases drastically the original wall wave height, but further increases in sill height act counter to their original reduction effects.

Fig. 31.

2. Wall Profiles:

Table I. summarized the maximum wall wave heights for the seven best series of sills tested. Fig. 32 is a plot showing the inside and outside wall profiles for the untreated channel under various conditions of discharge. Note that the flow patterns are all similar, the maximum points increasing considerably with discharge, while moving downstream only slightly. Figures 33, 34, 35, and 36 show these same wave patterns (for untreated flow) at discharges of 4.0, 3.0, 2.0, and 1.0 cu.ft. per sec., respectively. The graph of Fig. 37 shows the effects on wall profiles of variations in sill heights where the sills in each series are all the same. Note the comparison with untreated flow.

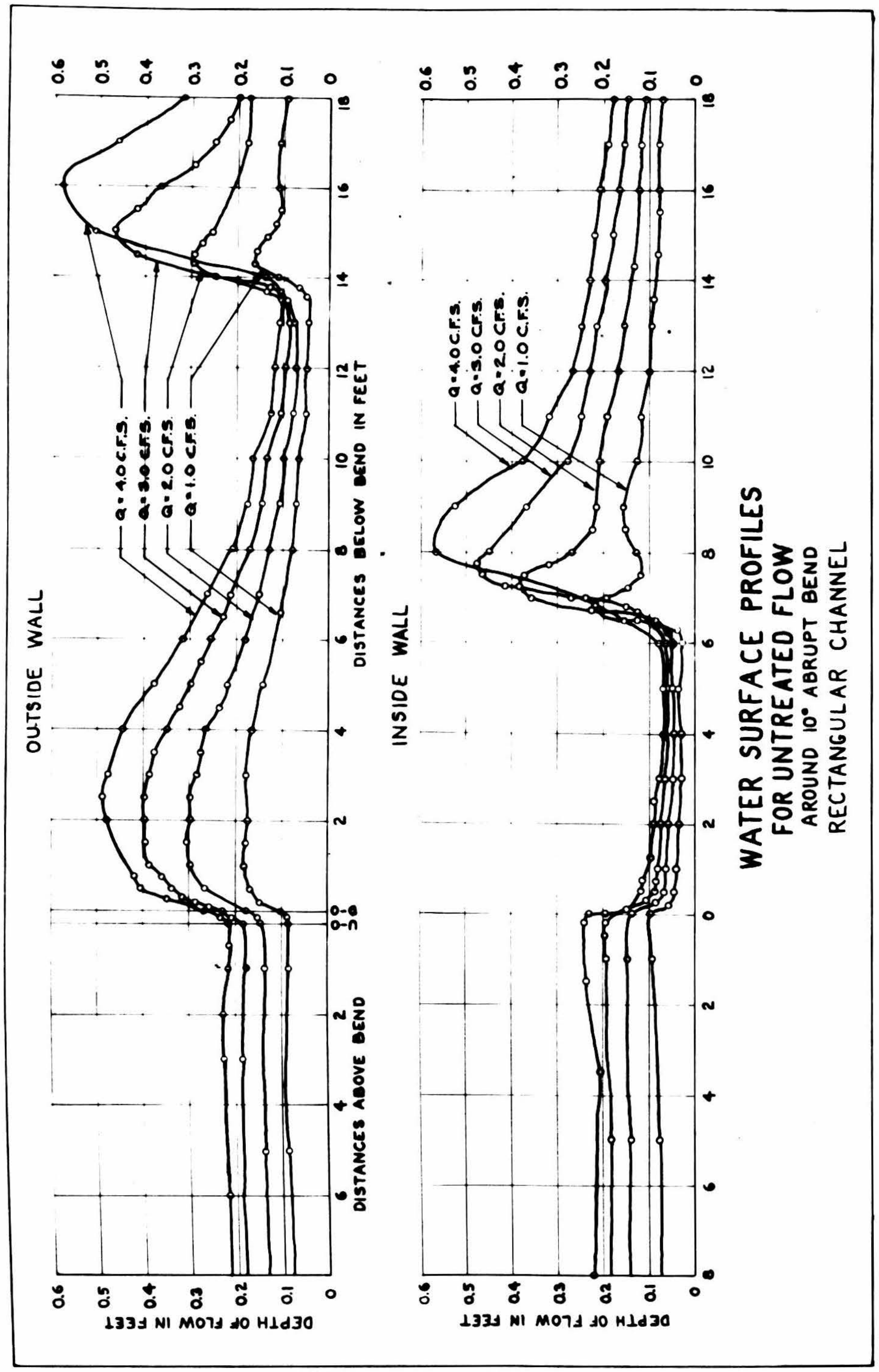
OUTSIDE WALL
INSIDE WALL
DEPTH OF FLOW IN FEET
DISTANCES ABOVE BEND
DISTANCES BELOW BEND IN FEET
Q = 4.0 C.F.S.
Q = 3.0 C.F.S.
Q = 2.0 C.F.S.
Q = 1.0 C.F.S.
WATER SURFACE PROFILES
FOR UNTREATED FLOW
AROUND 10° ABRUPT BEND
RECTANGULAR CHANNEL

Fig. 32.

Fig. 33.
Q = 4.0 cu.ft. per sec.

Fig. 34.
Q = 3.0 cu.ft. per sec.

Fig. 35.
Q = 2.0 cu.ft. per sec.

Fig. 36.
Q = 1.0 cu.ft. per sec.

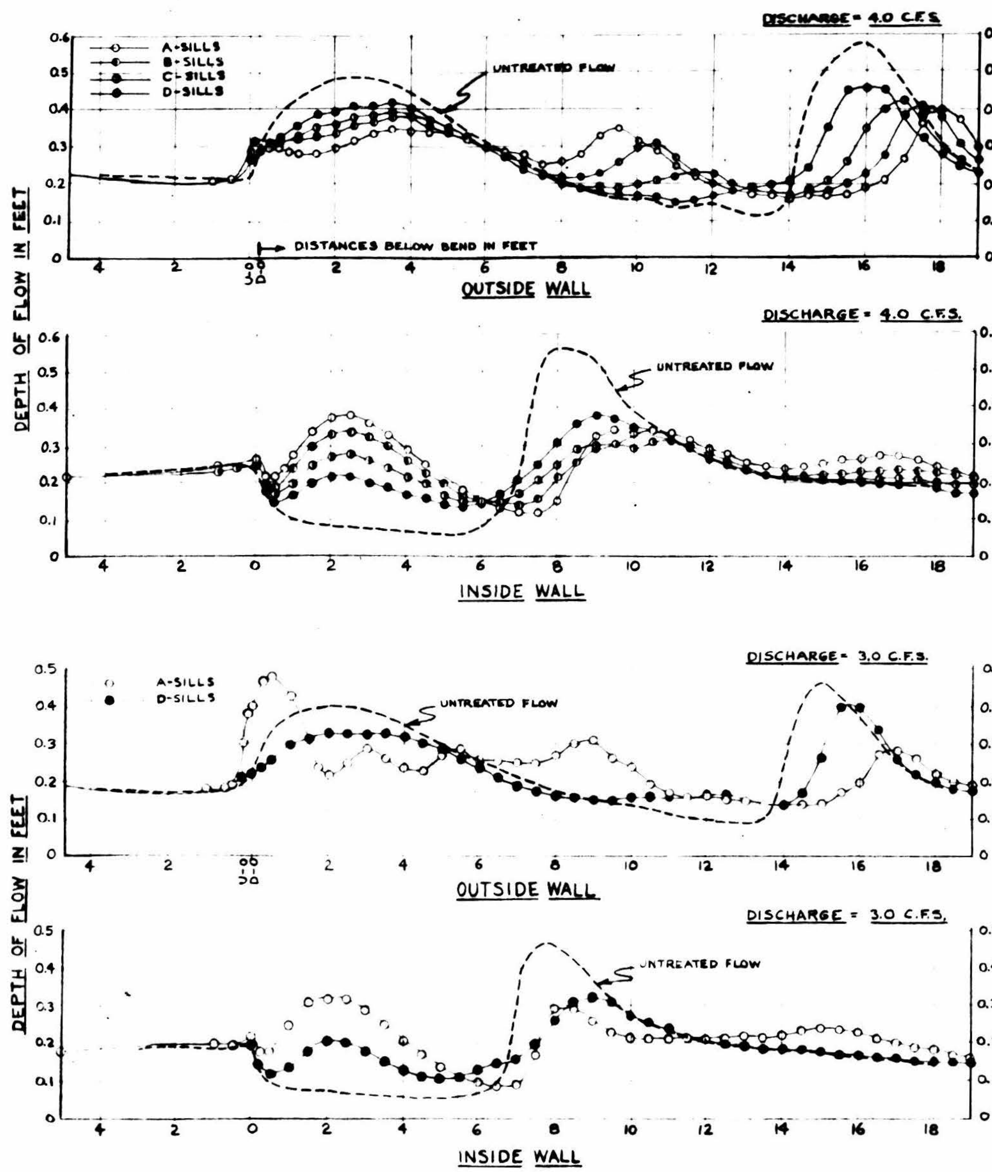

WATER SURFACE PROFILES FOR TREATED FLOW (UNIFORM-SIZED SILLS)

AROUND A 10° ABRUPT BEND IN RECTANGULAR CHANNEL

Fig. 37.

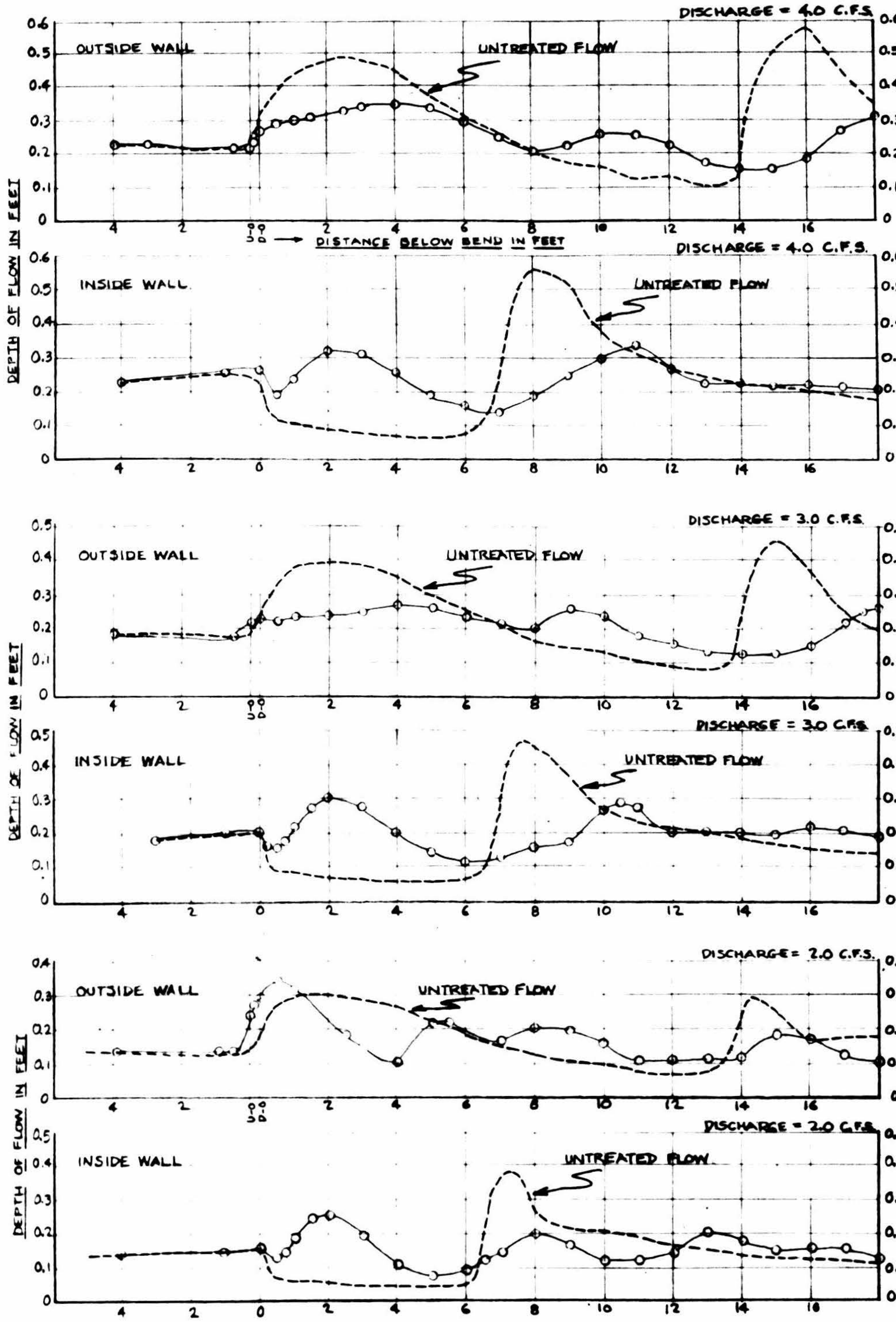

WATER SURFACE PROFILES FOR TREATED FLOW (K-SILLS)
AROUND A 10° ABRUPT BEND IN RECTANGULAR CHANNEL

Fig. 38.

Fig. 38 is a graph comparing the wall profiles for the best treatment found with those for the untreated channel. A comparison of three types of treatment versus no treatment for 4.0 cu.ft. per sec. are shown on page 61. Fig. 39 is for no treatment, Fig. 40 for treatment with K-sills, Fig. 41 for treatment with I-sills, and Fig. 42 for treatment with A-sills. For this quantity of discharge it is apparent that the I-sills offer the best corrective prospects. Figures 43, 44, 45, and 46 are the same conditions except for the discharge being 3.0 cu.ft. per sec. The actions of these sills under a discharge of 2.0 cu.ft. per sec. is shown in Figures 47, 48, and 49, where Fig. 47 is for the untreated channel, Fig. 48 is for K-sills, and Fig. 49 is for A-sills. The effects of the I-sills are almost identical with those of the A-sills.

Attention is called to the very undesirable flow conditions over the A-sills shown in Fig. 49. It was this same feature of the I-sills which prevented their being the best selection. Although this condition appears to exist for the K-sills in Fig. 48, the offense is not serious because it only occurs in an unfavorable degree on sills Nos. 2 and 3, and has no undesirable effect on the outside wall. The angle at which the picture was taken does not permit a view of the action over sill #1. The splashing actually is more of the magnitude of that over sill #4. Confirmation of this fact can be made by referring to Fig. 75 , which is an upstream view for a similar condition of flow. It can be seen that no objectionable splashing takes place at the wall, due, undoubtedly,

Fig. 39.
No Treatment
Q = 4.0 cu.ft. per sec.

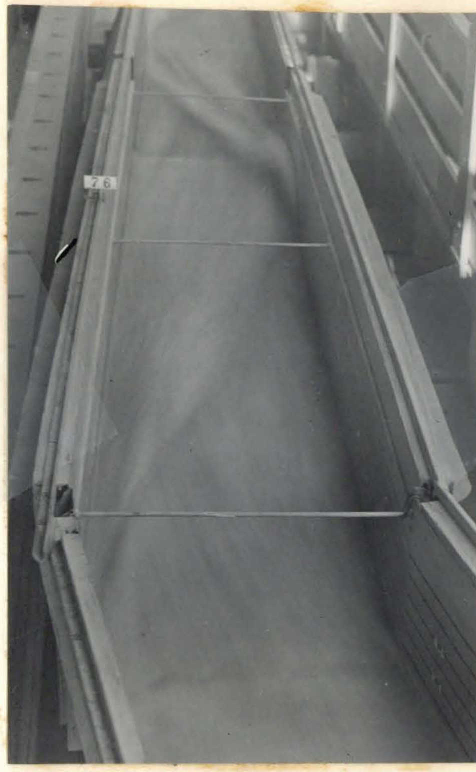

Fig. 40.
K-sills
Q = 4.0 cu.ft. per sec.

Fig. 41.
I-sills
Q = 4.0 cu.ft. per sec.

Fig. 42.
A-sills
Q = 4.0 cu.ft. per sec.

Fig. 43.
No Treatment
Q = 3.0 cu.ft. per sec.

Fig. 44.
K-sills
Q = 3.0 cu.ft. per sec.

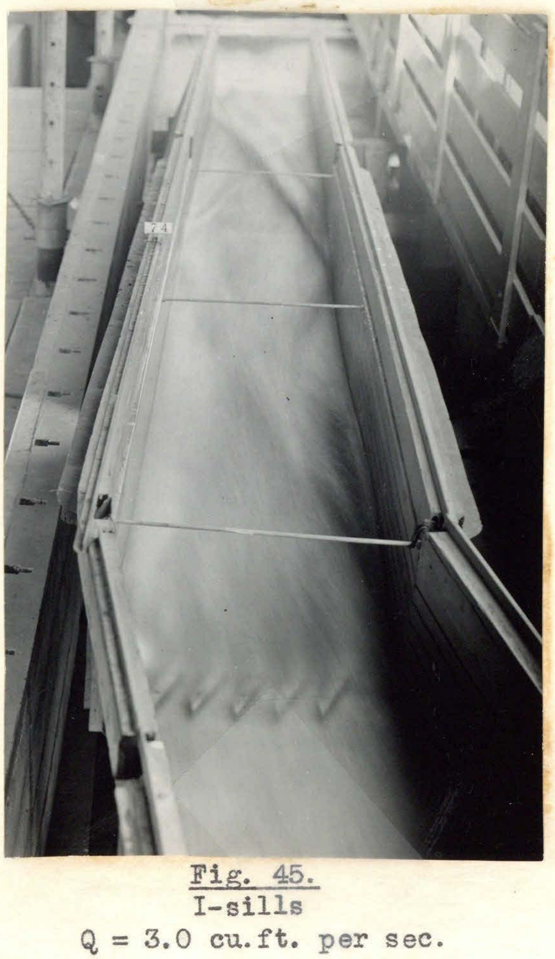

Fig. 45.
I-sills
Q = 3.0 cu.ft. per sec.

Fig. 46.
A-sills
Q = 3.0 cu.ft. per sec.

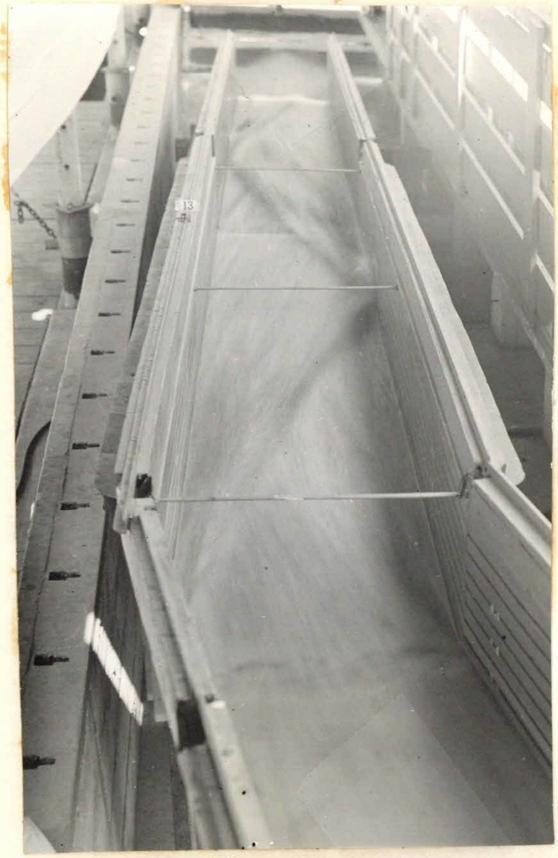

Fig. 47.
No Treatment
Q = 2.0 cu.ff. per sec.

Fig. 48.
K-sills
Q = 2.0 cu.ft. per sec.

Fig. 49.
A-sills
Q = 2.0 cu.ft. per sec.

to the lower #1 sill height and its location near the wall. Verification of this can also be seen by reference to Fig. 29, where sill #1 is even there splashing considerably less than the others.

Fig. 50.

Prohibitive wall water heights due to such splashing over the I-sills led to their rejection as a satisfactory corrective means, regardless of their superior performance over all the other sills at higher discharges, K-sills included.

Fig. 50 shows the first maximum wave on the inside wall for Q = 4.0 cu.ft. per sec. (untreated flow) before the addition of the ten foot downstream section. Thorough investigation of wall profiles for various fillets placed at the bend revealed that the fillet had little effect. Fillets with radii of 18 inches, 36 inches and 54 inches were formed by plasticene so as to obtain a smooth and even transition around the outside wall.

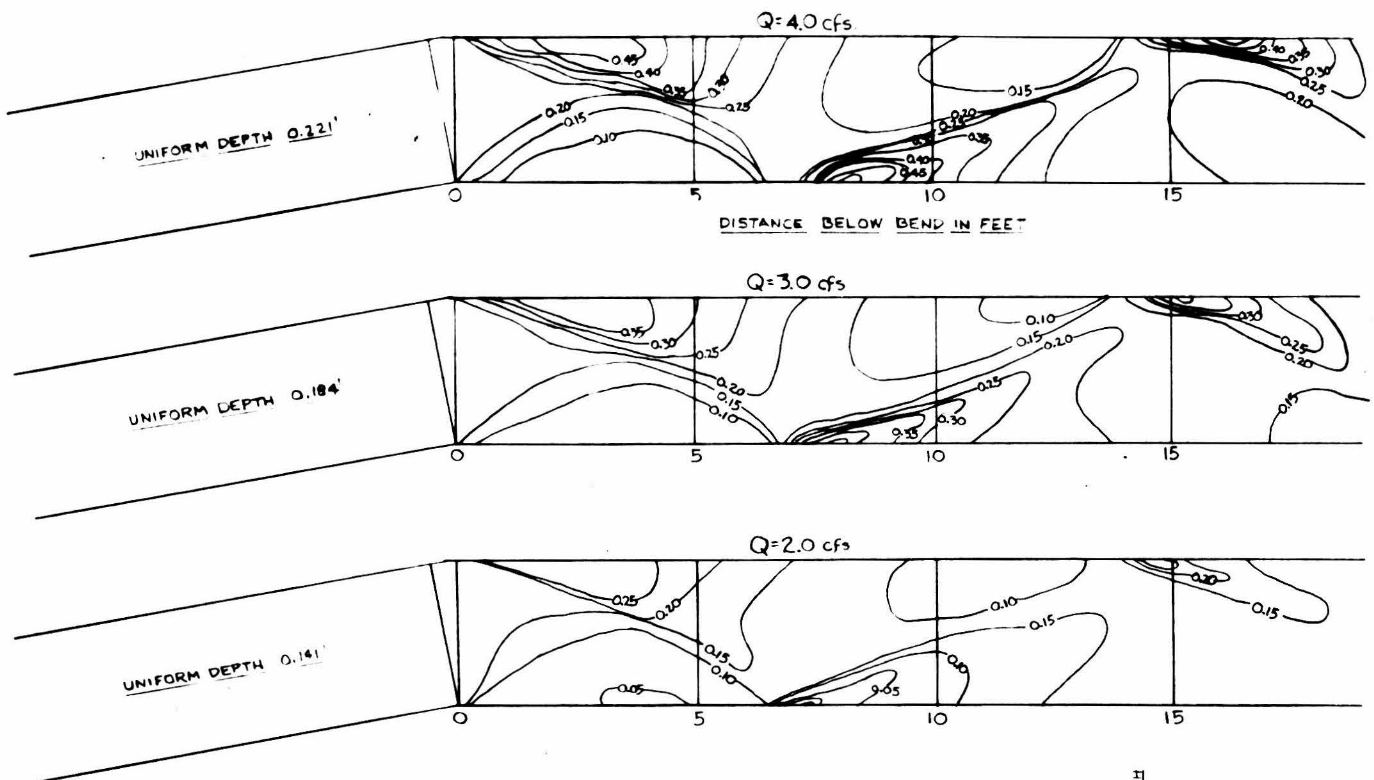

WATER SURFACE CONTOURS
FOR UNTREATED FLOW
AROUND 10° ABRUPT BEND
RECTANGULAR CHANNEL

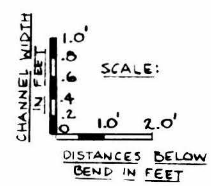

Fig. 51.

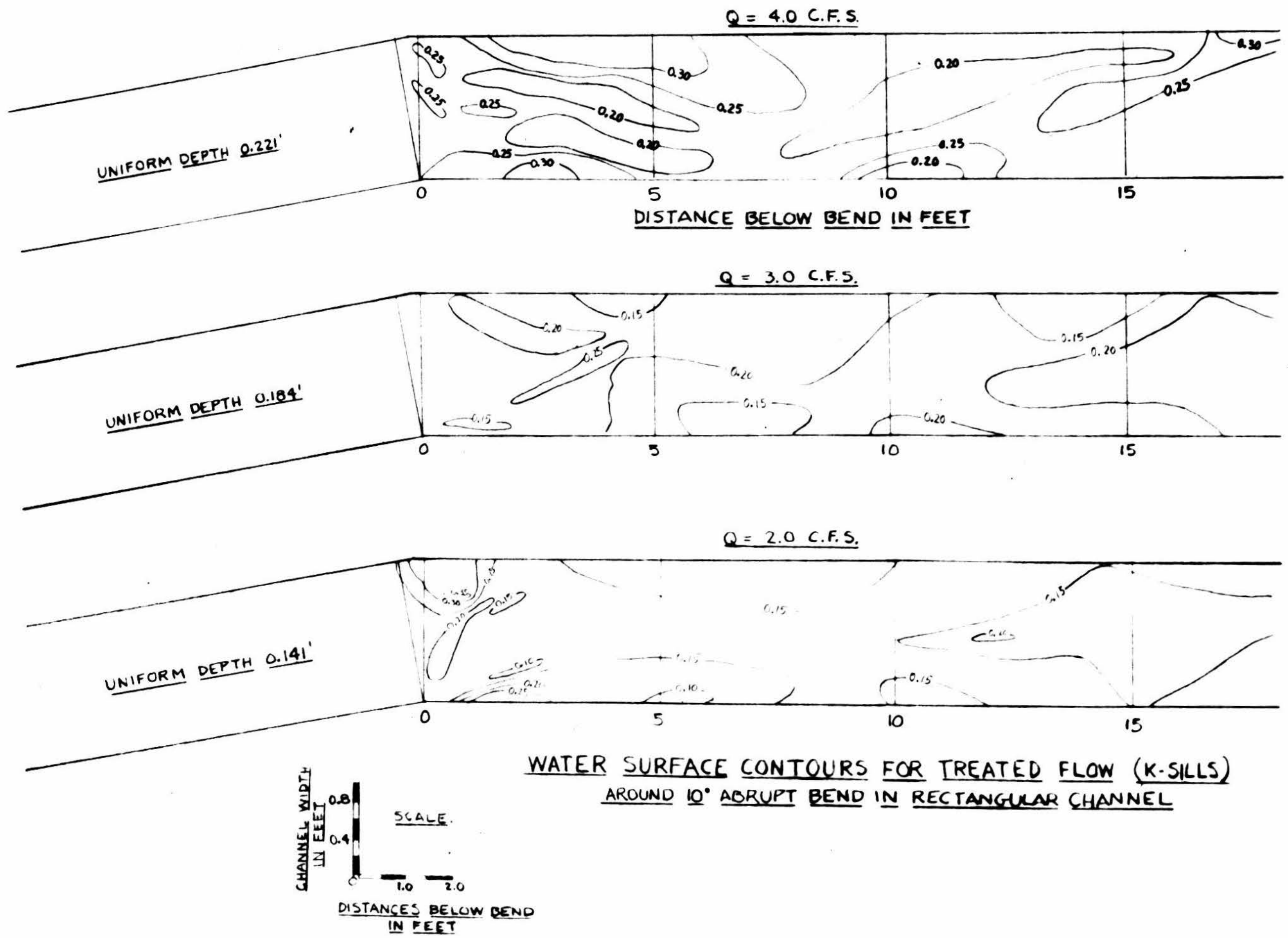

WATER SURFACE CONTOURS FOR TREATED FLOW (K-SILLS)
AROUND 10° ABRUPT BEND IN RECTANGULAR CHANNEL

Fig. 52.

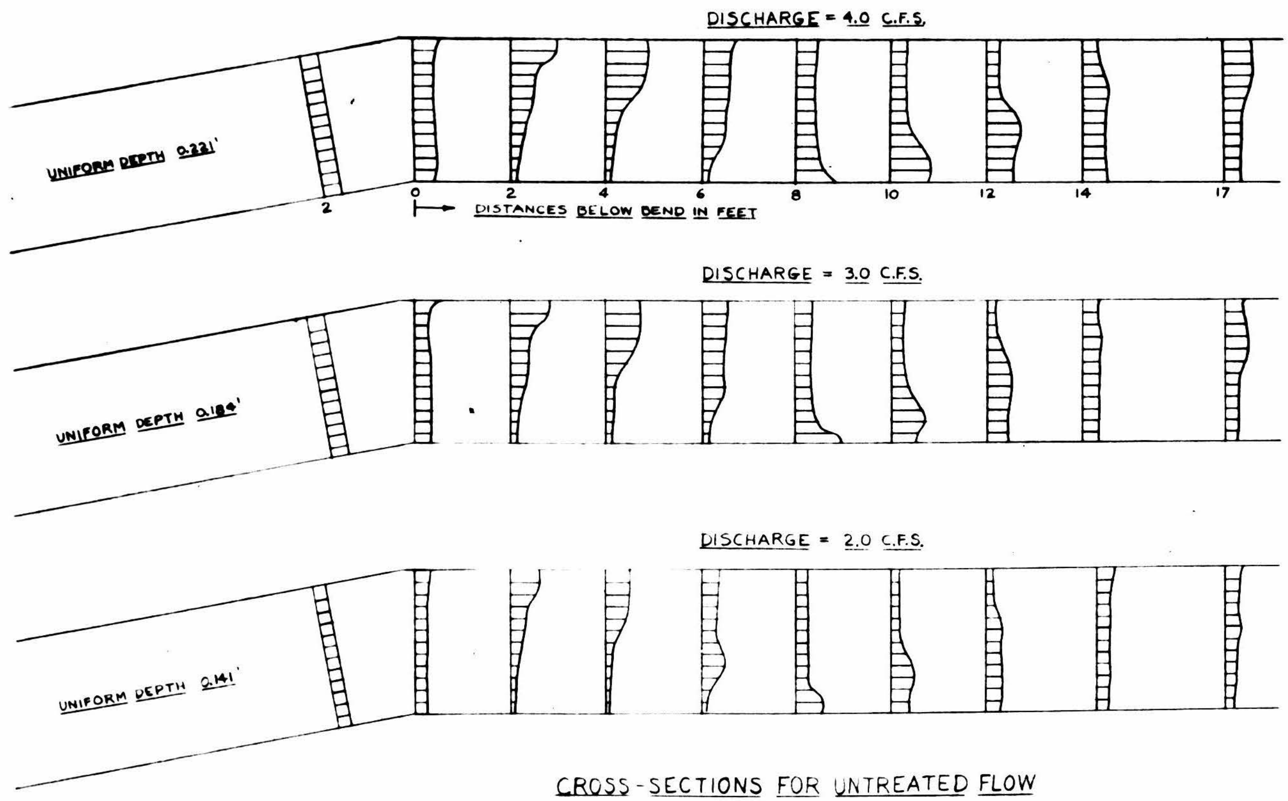

CROSS-SECTIONS FOR UNTREATED FLOW
AROUND 10° ABRUPT BEND IN RECTANGULAR CHANNEL

Fig. 53.

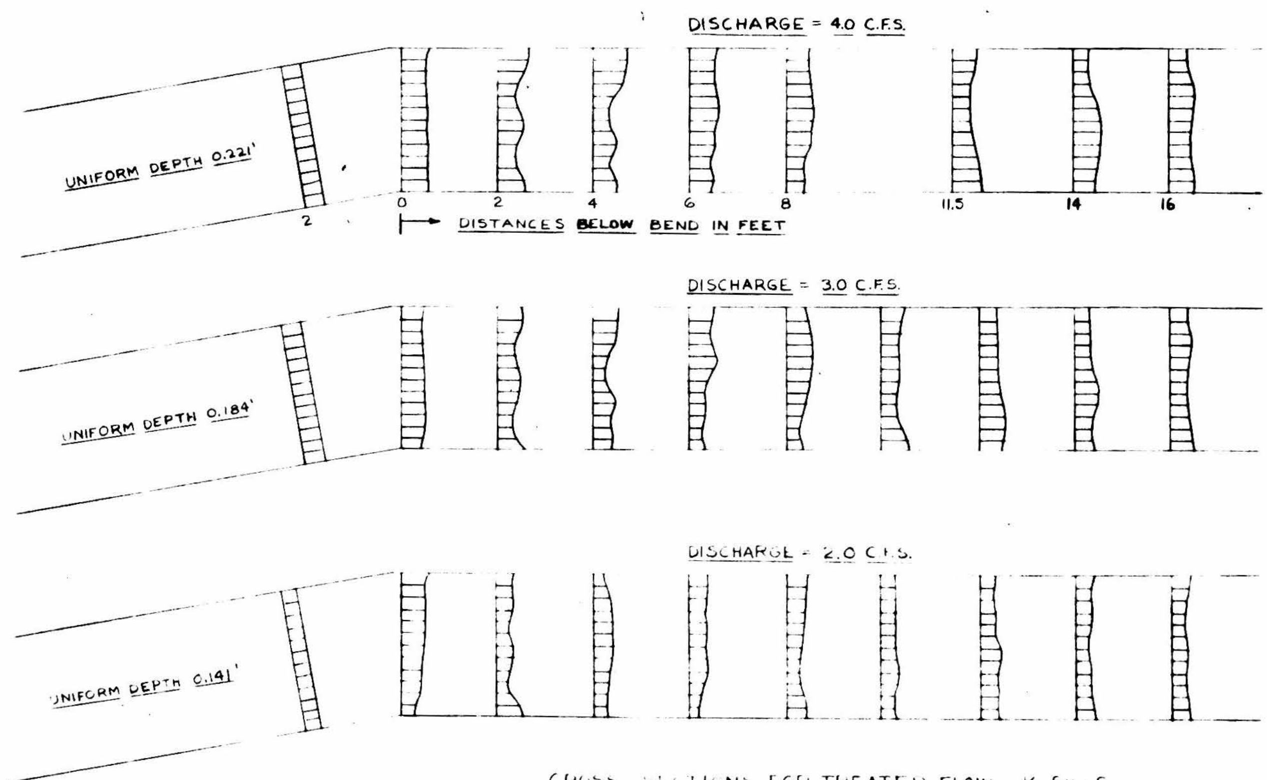

CROSS SECTIONS FOR TREATED FLOW - K-SILLS
AROUND 10° ABRUPT BEND IN RECTANGULAR CHANNEL

Fig. 54.

3. Water Surface Contours:

All of the photographic views of the previous section apply also to this section as they indicate not only the wall profiles, but also the variations existent over the water surface within the channel. Contours of equal depths showing the magnitudes of the wave crests and troughs have been plotted for several different types of treatment. Those for untreated flow conditions may be seen in Fig. 51, while those for the best treatment are found in Fig. 52. Note the drastic reduction of peaks at the three wave crossing points with the K-sills. Changes in water surface from one section to another are best typified by the cross-section comparison of Fig. 53 and Fig. 54 for the same flow conditions just described.

4. Velocity Distribution:

Comprehensive velocity studies were made only for the maximum rate of discharge for both the untreated channel and for the treat-

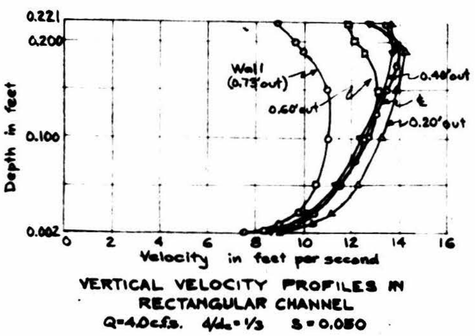

Fig. 55.

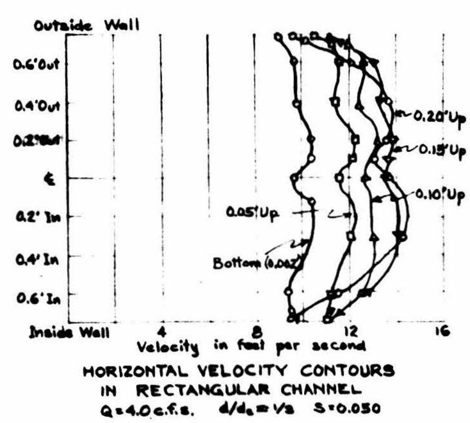

Fig. 56.

ment with K-sills because of the length of time required for this study at each cross-section. Approximately half a day was devoted to each, several weeks being required to complete the study. Typical vertical and horizontal velocity profiles are shown in Fig. 55 and Fig. 56. Velocity distribution throughout various cross-sections are shown in Fig. 57 and Fig. 58, the former indicating that for the untreated channel, the latter that for the best treatment.

Fig. 59 is a very interesting study of velocity distribution immediately downstream from the K-sills (Q = 4.0).

Velocity vectors; i.e., magnitude and direction, in a horizontal plane are illustrated in Fig. 60, Fig. 61, and Fig. 62. Fig. 60 portrays conditions at various depths above the channel bottom just downstream from the K-sills, at the same location shown in Fig. 59.

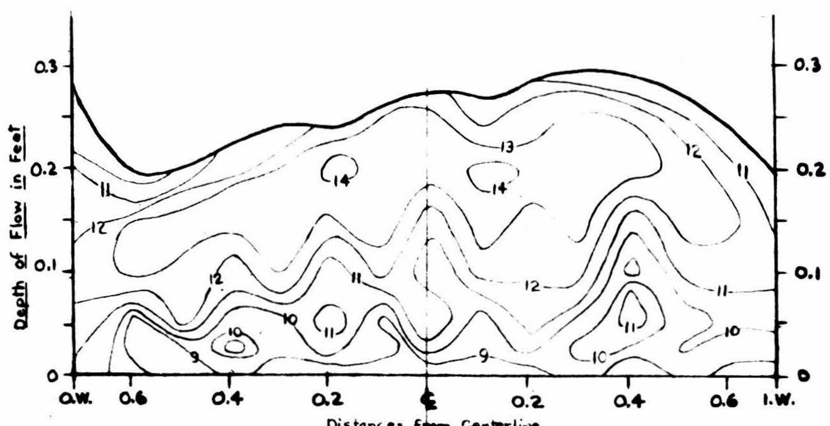

VELOCITY DISTRIBUTION IN CHANNEL
CROSS-SECTION JUST DOWNSTREAM FROM K-SILLS
Q = 4.0 C.F.S.

Fig. 59.

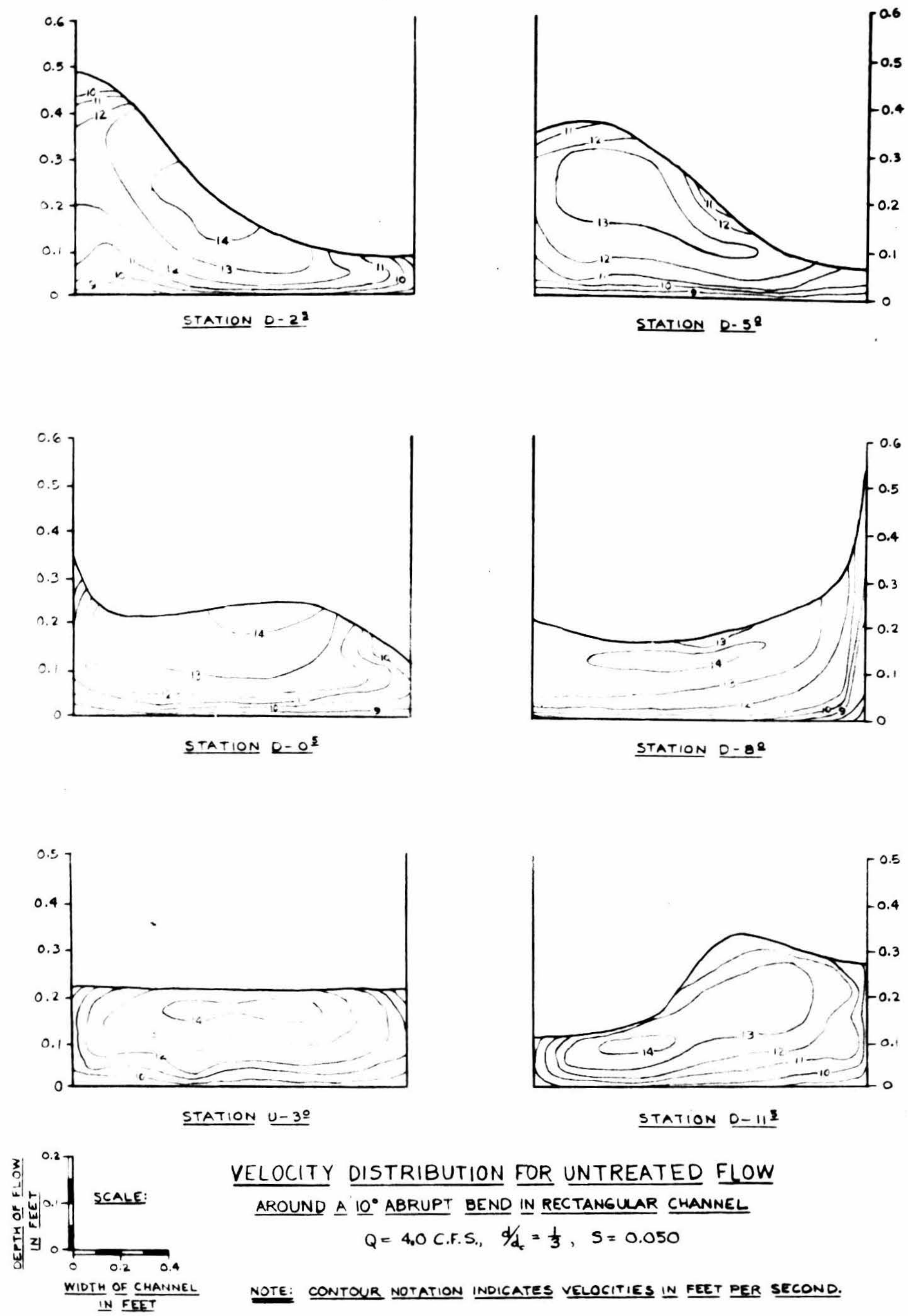

VELOCITY DISTRIBUTION FOR UNTREATED FLOW
AROUND A 10° ABRUPT BEND IN RECTANGULAR CHANNEL
$Q = 4.0$ C.F.S., $d/d_c = \frac{1}{3}$, $S = 0.050$

NOTE: CONTOUR NOTATION INDICATES VELOCITIES IN FEET PER SECOND.

Fig. 57.

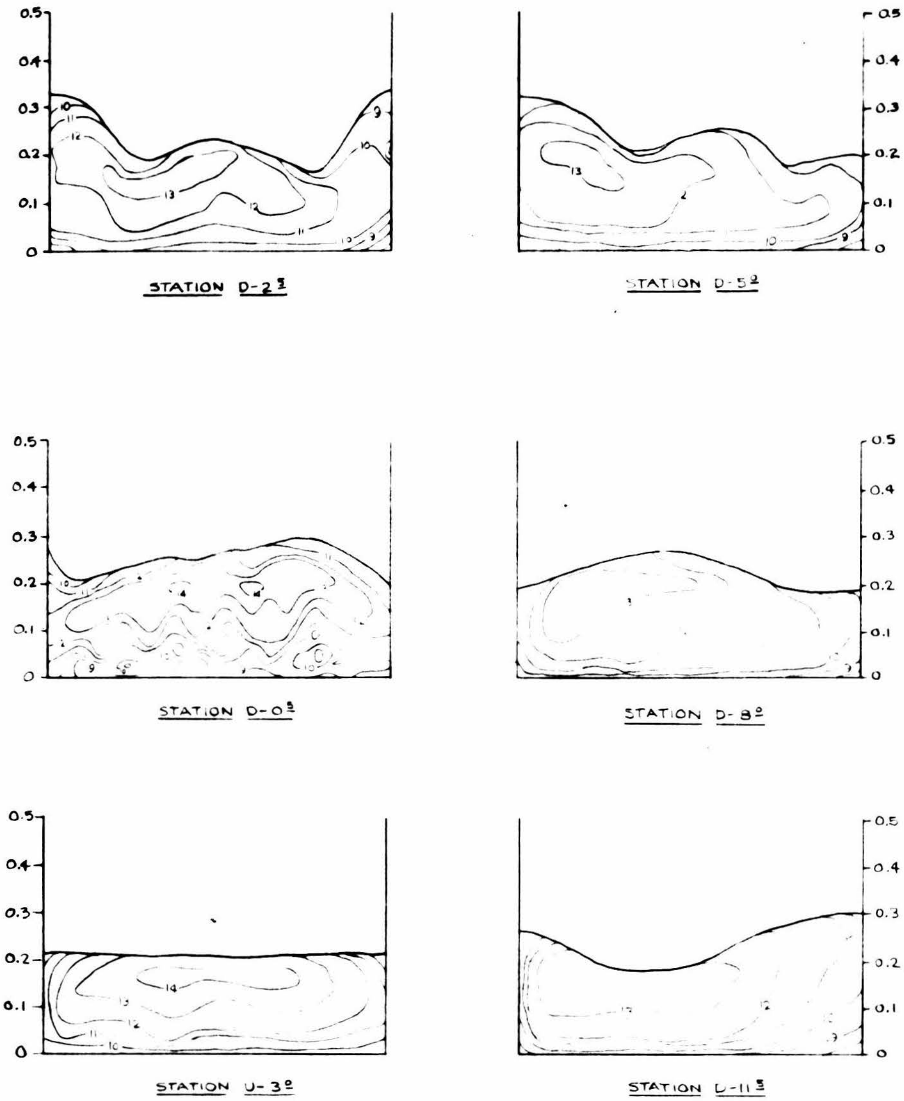

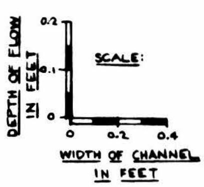

VELOCITY DISTRIBUTION FOR TREATED FLOW (K-SILLS)

AROUND A 10° ABRUPT BEND IN RECTANGULAR CHANNEL

$Q = 4.0$ C.F.S., $y/d_c = \frac{1}{3}$, $S = 0.050$

NOTE: CONTOUR NOTATION INDICATES VELOCITIES IN FEET PER SECOND

Fig. 58.

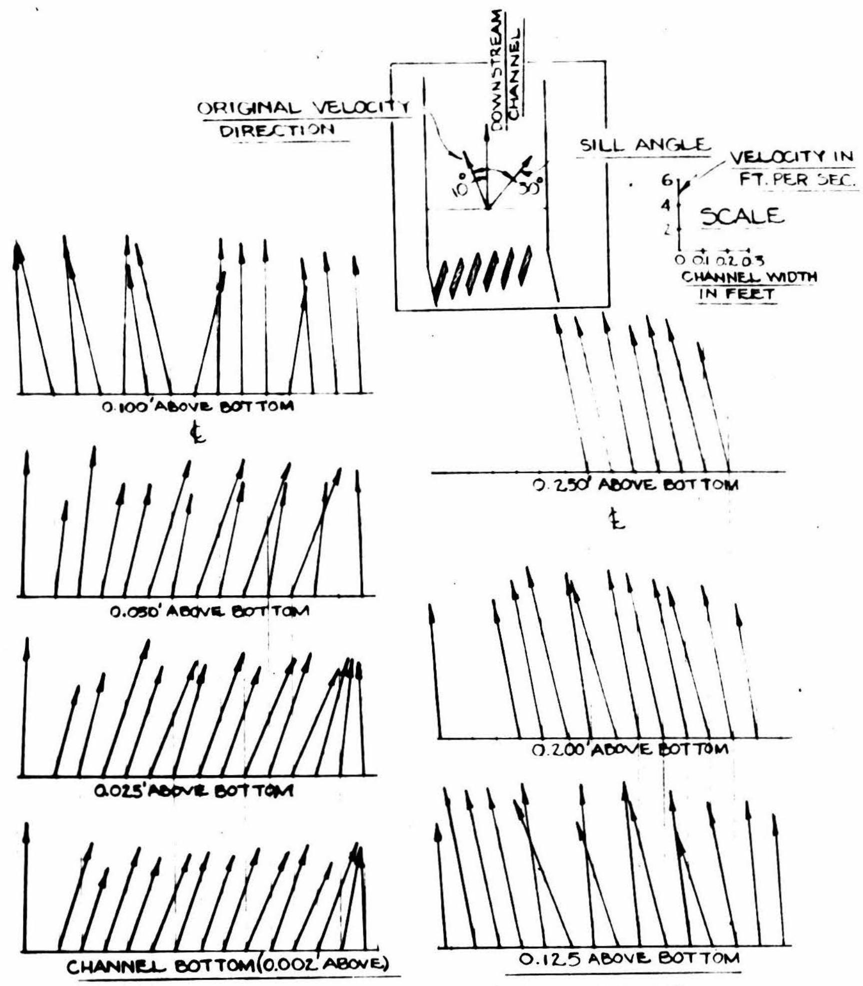

HORIZONTAL VELOCITY VECTORS AT STATION D-0^5 FOR K-SILLS Q = 4.0 cfs

Fig. 60.

The directions of the lines represent the velocity directions as measured and the length of the lines represent magnitudes as measured. Note how effectively the sills divert the water without

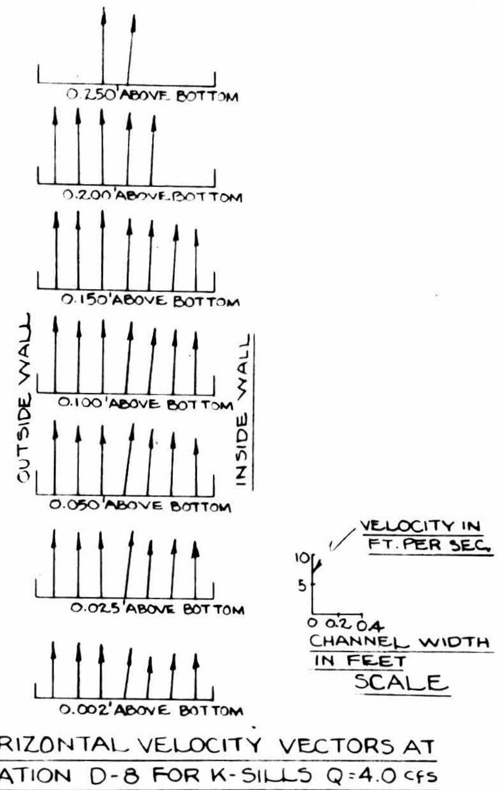

Fig. 61.

destroying the nearly uniform velocity magnitude. Fig. 61 portrays conditions at Station D-8 with the same set of sills and the same discharge. Fig. 62 shows the bottom velocity vectors at different stations throughout the channel.

5. Momentum Changes:

Table II. is a summary of the average forces exerted on several series of sills for various discharges. As previously mentioned, the sill plate was surprisingly free in its movements, giving consistent readings for any set of conditions. Note the similarity of force components for certain sill types.

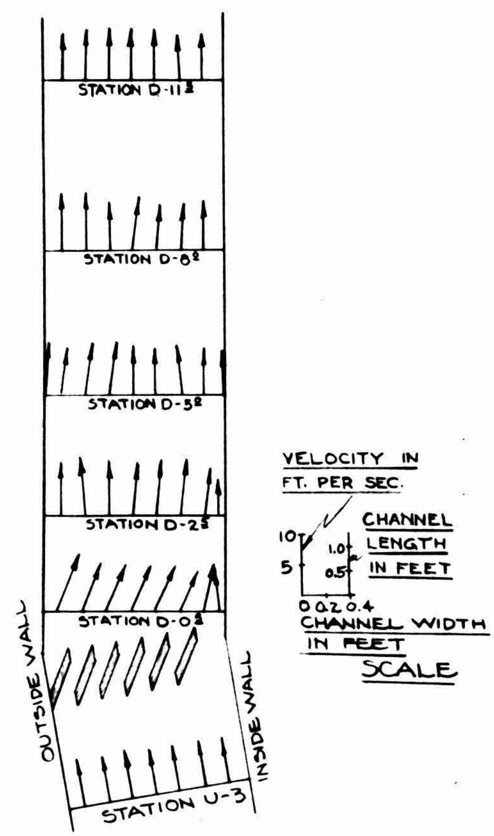

BOTTOM VELOCITY VECTORS
K-SILLS Q = 4.0 cfs.

Fig. 62.

TABLE II.

Summary of Force Measurements (in lbs.)

Sill Series	Dis-charge	P_y Scale No. 3	P_{x1} Scale No. 4	P_{x2} Scale No. 5	P_x $P_{x1} + P_{x2}$
B	4.0	9.63	3.38	4.63	8.01
	3.0	7.63	2.44	3.81	6.25
	2.0	5.38	1.50	2.75	4.25
C	4.0	7.56	2.56	3.94	6.50
	3.0	6.00	2.13	3.06	5.19
	2.0	4.56	1.13	2.25	3.38
K	4.0	9.63	3.56	4.69	8.25
	3.0	7.50	2.19	3.81	6.00
	2.0	5.44	1.50	2.69	4.19
I	4.0	10.13	2.88	4.88	7.76
	3.0	7.63	2.25	3.94	6.19
	2.0	5.63	1.19	2.94	4.13
A	4.0	11.19	3.63	5.81	9.44
	3.0	9.19	2.31	5.00	7.31
	2.0	7.19	1.94	3.75	5.69

IV. COMPARISON OF ANALYTICAL AND EXPERIMENTAL RESULTS

A. UNTREATED FLOW

1. Wave Depths:

In the analytical development of the two simultaneous Equations (27) and (30), it was assumed that the sections of fluid under consideration were sufficiently removed from the wall to insure full development of the shock wave. It would, therefore, be illogical to expect these shock wave equations to indicate the depth of flow along the walls. Because of the nearness of the wave front to the outer wall, the condition of uniform flow on the downstream side (or d_2 side) cannot be fulfilled. The influence of the outer wall would, undoubtedly, be anticipated to be an additive one, giving values higher than would be obtained by the shock wave formula. Table III. confirms this. With lower discharges, and, accordingly, lower depths of uniform flow, conditions become nearer and nearer those assumed, and it is to be expected that the shock wave development could proceed unhampered without too much wall influence. Accordingly, the wave formula should give a better approximation to the actual depths. In Table III. the analytical values of d_2 do approach more nearly those experimentally obtained. In all runs the water along the outside wall piles up rapidly and give s the appearance of folding over the water beneath it similar to the folds of a ribbon.

Fig. 64 shows details of the flow along the outside wall in the vicinity of the bend (Q = 4.0). Although this picture does not show

TABLE III.

Comparison of Wave Depths and Locations

Untreated Flow

Item	Symbol	Discharges in cu.ft. per sec.			
		4.0	3.0	2.0	1.0
Uniform Depth	d_1	0.221	0.184	0.141	0.091
Shock Wave Depth (Anal.)	d_2	0.424	0.353	0.271	0.175
First Max. Wall Depth (Exp.)	d	0.487	0.388	0.298	0.180
% Excess Over Shock Depth		15%	10%	6%	3%
Negative Wave I.W. (Anal.)	d_2	0.088	0.074	0.056	0.036
Min. Inside Wall Depth (Exp.)	d	0.068	0.060	0.044	0.025
Ave. Area Depth Below Wave (Exp.)	d_2	0.085	0.075	0.060	0.031
Location First Max. (I.W.) (Anal.)	R_{in}	6.92	6.92	6.92	6.92
Location First Max. (I.W.) (Exp.)	R_{in}	8.0	7.5	7.2	7.0
% Difference (Anal. to Exp.)		12%	8%	4%	1%
Location Min. I.W. Depth (Exp.)		6.4	6.3	6.2	6.1
Wave Length (Anal.)	L	13.8	13.8	13.8	13.8
Wave Length (Exp.)	L	13.5	13±	13±	13.5±
% Difference (Anal. to Exp.)		2%	6%	6%	2%

it too well, at large discharges considerable air is entrained at the wave front by the folding effect and is carried on downstream with the flow.

Table III. also gives a comparison of the minimum wave depths as determined analytically with the experimentally determined minimum wall depths, which again, as discussed above, could not be expected to be typical of the depths to be encountered just below the wave. For that reason the average depths in the fairly extensive area below the negative wave front have been listed for comparison. These should compare well with analytical values and they do. This area can be seen quite clearly in Fig. 66. Note the extensiveness of it. Attention is also called to the rapid drop in water surface along the inside wall as the water passes around the bend. To the left can be seen quite clearly the "ribbon-like" folding over of the water as the positive wave reaches the inside wall downstream from the bend and is reflected to the other side again. Further confirmation of the extent of this "hollow area" is also obtained from the water surface contours of Fig. 51.

Fig. 63 is a view looking almost directly down at the wave front when the discharge is only 1.0 cu.ft. per sec. It is obvious that the wave front does not lie along a straight line, but curves outwardly as it progresses downstream in accord with previous analytical developments;(i.e., increases in depth of water augment the wave celerity, as shown by Equations (7) and (19), with a resultant effect of enlarging the cross-component of the vector-velocity relationship between C and V).

Fig. 63.

2. Location of Wave Crossings:

Table III. includes a comparison of the analytical and experimental locations of the wave crossings. The agreement is not too good at the higher discharges, 12% difference for a discharge of 4.0 cu.ft. per sec., and 8% for 3.0 cu.ft. per sec. However, as the discharge decreases, which, in turn, indicates an upstream depth decrease, the percentage disparity between analytic and measured values also decreases.

Precise determination of the wave length is difficult experimentally unless the downstream channel is sufficiently long to enable measurement of several wave lengths. The chief difficulty is in selecting the location of the maximum water height along the channel wall because the water surface profile is a broad flat curve in this region. Nevertheless, analytical and experimental agreement was remarkably close, as shown by the figures in Table III. Fig. 32 shows this tendency toward broad, flat peaks, and also emphasizes the fact that maxima and minima locations shift only slightly with changes in discharge.

3. Velocity Distribution:

The assumption of uniform velocity throughout the cross-section is an exceedingly good one. In Fig. 55 the velocity profiles taken through vertical sections parallel to the channel walls at the center-line, 0.2 ft. out, 0.4 ft. out, and 0.6 ft. out practically lie on top of each other, and the wall profile, 0.73 ft. out, is made up of velocities sufficiently large in magnitude to fulfill the uniform velocity criteria within the accuracies of the limitations set. Likewise, the horizontal velocity profiles, Fig. 56, fall within a narrow range, only the extreme bottom velocity differing from the others. The bottom velocities, as previously mentioned, are within 0.002 ft. of the channel bottom. Fig. 57 confirms the assumption of relatively constant velocity in the downstream section. In this regard, the latter plot is an interesting study of the changes in velocity distribution as the water flows through the channel. Changes in cross-sectional shape and area are rapid and violent.

B. TREATED FLOW

1. Wall Wave Heights:

The principal requirement of a perfect wave repression device is the ability to reduce the wave peaks immediately below the bend and in the downstream section, and to increase the wave troughs to such a value that uniform downstream wall height will result. One would expect such a corrective device to be extremely complicated because of the multitudinous corrective features it would have to entail. Thinly-constructed, closely-spaced, confining walls or vanes within the bend might serve to re-develop fairly uniform downstream conditions, although the height to which the water would rise along these vanes would approximate that along the outer wall without vanes. Construction difficulties would not be the only disadvantageous factor in their use. They would not have the ability to insure passage of debris down the channel unless the maximum linear dimension of any foreign material in the water were less than the clear passage distance between any two walls, not an assured condition.

Although no corrective devices studied in this research approached closely the ultimate in perfection, many served as a feasible and practicable means of reducing drastically the unwanted and highly undesirable wave heights present in the untreated channel. Early in the experimental studies, it was found that echelon-type sills had great possibilities and rapidly eliminated other means of correction. Experimentation with many types, sizes, and shapes gradually eliminated all but a few, and of these few, one stood out above the others as giving the best corrective measures. As previously mentioned, these were the K-sills, pictured in Fig. 30. Comprehensive examination of their characteristics was conducted over a wide range of discharges, and, although far from perfect, they should, nevertheless, serve as entirely satisfactory wave repressing devices. Fig. 38 is a comparative plot of the effect of K-sills on wall water heights downstream from the bend. Note the very favorable reduction in maximum wall heights, the K-sills reducing this height to never more than a value of 0.34, as against untreated flow heights of 0.58 on both outside and inside wall when the discharge is 4.0 cu.ft. per sec. At lower discharges, the K-sills still keep the maximum wall height below the 0.34 value. These sills also have the effect of filling up the wave troughs on both the inside and outside wall. Their effectiveness in repressing the outside wall wave height just below the bend can best be realized by reference to Fig. 64 and Fig. 65, the former figure having been referred to in previous sections. The inside wall effects can be seen in Fig. 66 and Fig. 67. Note in Fig. 67 the increased, yet not unfavorable, height to which the sills build up the water along the inside wall and the outstanding lack of the high cross-wave at the left of the picture. As can be seen in the plot of Fig. 38, the inside wall maximums are those most drastically reduced. A comparative view of the cross-sections at various stations along the channel with and without K-sills are seen in Fig. 54 and Fig. 53. Those under the influence of the

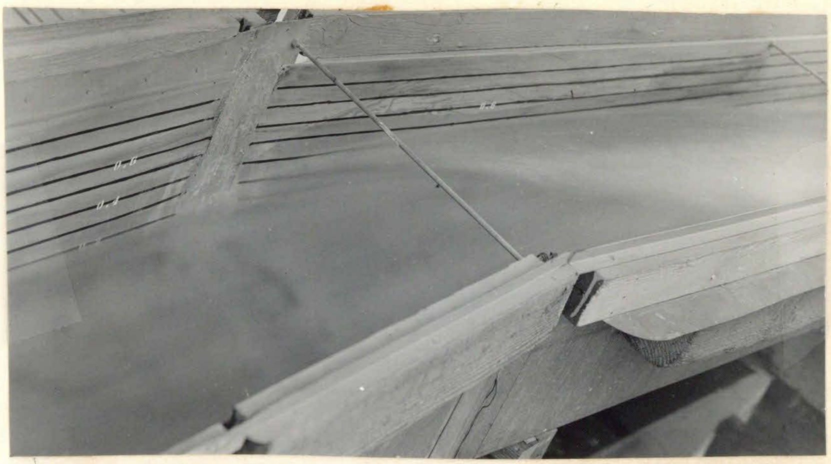

Fig. 64.

Fig. 65.

K-sills are much more regular in form. Still another comparison can be seen in Fig. 51 and Fig. 52, where lines of equal water height are plotted to give a contour map of the water surface with no treatment and with the K-sills acting.

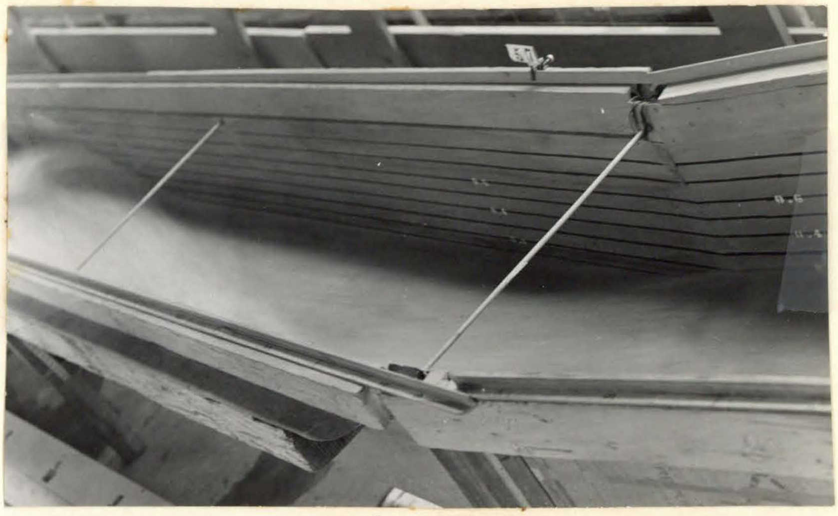

Fig. 66.

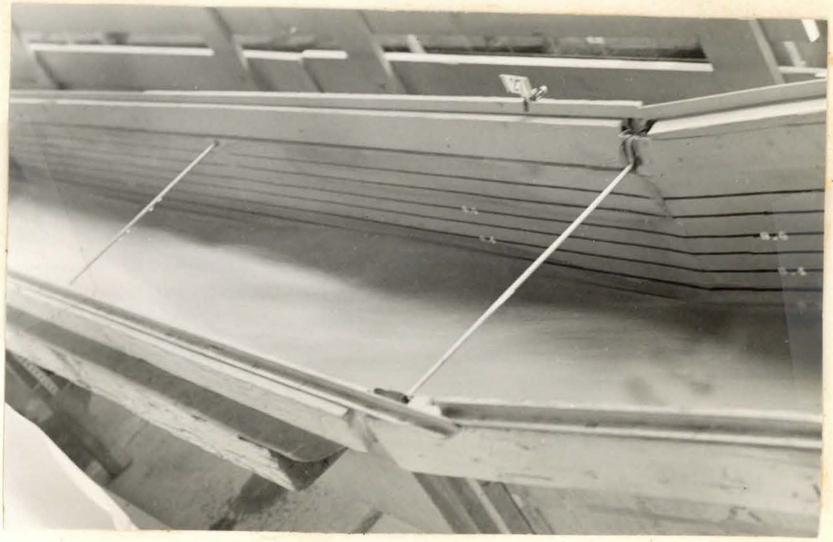

Fig. 67.

TABLE IV.

Item	Q = 4.0 cu.ft. per sec.		Q = 3.0 cu.ft. per sec.	
	Untreated Flow	With K-sills	Untreated Flow	With K-sills
Uniform Depth, d_1	0.221	0.221	0.184	0.184
First Max. Depth, O.W.	0.487	0.340	0.400	0.264
Second Max. Depth, I.W.	0.566	0.332	0.473	0.288
Third Max. Depth, O.W.	0.576	0.340	0.462	0.261
Highest Max. less d_1	0.355	0.119	0.278	0.077
Percent Max. K to Untreated Max.	100%	33.5%	100%	27.8%
First Min. Depth, I.W.	0.069	0.140	0.056	0.113
Second Min. Depth, O.W.	0.110	0.155	0.085	0.127
d_1 less Lowest Min.	0.152	0.081	0.128	0.057
Ratio-K to Untreated Min.	100%	53%	100%	45%

Table IV. compares the pertinent changes in wall water heights occasioned by the induced action of the K-sills. The K-sills reduce the maximum wall depths to only 33.5 percent of the worst possible conditions for a discharge of 4.0 cu.ft. per sec. and to only 27.8 percent for a discharge of 3.0 cu.ft. per sec. At the same time they build up the minimum depths to a point such that the drop in depth with K-sills is only 53% that for untreated flow at 4.0 cu.ft. per sec. and 45% that at 3.0 cu.ft. per sec. As previously discussed, additions to low depths are desirable but certainly are of minor significance compared to the lowering of the maxima. For an excellent comparison of the effects of the K-sills throughout a wide range of discharges, refer to the photographic study contained in Figures 68 through 75, which will be discussed in a later section.

2. Velocity Distribution and Reduction of Transverse Velocity:

The validity of the assumption of uniform velocity has been previously discussed. It is relevant to point out here, however, the comparative effects of the K-sills upon the velocity distribution at various downstream sections. Proceeding up the left side of Fig. 57, across the top, and down the right side, one can obtain an excellent idea of the shifting of the velocity distribution contours as the flow undergoes the severe changes caused by the bend and progresses on downstream. It is not difficult to visualize the bouncing of the waves back and forth across the channel for a considerable distance downstream. Throughout all this violent agitation, the flow manages to proceed with the same range of velocities at which it originally entered the bend. Nor do the sills have any great retardation effect, either immediately downstream or further downstream, as can be seen in Fig. 58. There are no areas of greatly reduced velocity, and by the time Station D-11.5 is reached, the velocity distribution pattern is rapidly returning to its normal upstream state. The components normal to the channel walls damp out rapidly. Fig. 61 is a schematic summary of a probe of the horizontal velocity vectors at various distances between the channel bottom (0.002 ft. above) and the water surface at a distance of eight feet downstream from the bend and the sills. Throughout the full depth the velocity on almost the entire outside half of the channel is now parallel to the channel walls, and such transverse velocity components as still exist are indeed small in magnitude. That the bottom water area downstream from the sill region has a rapid and effective influence on the upper area and vice versa, can be seen by reference to Fig. 60 and Fig. 61. In the former, the velocity vectors of the lower and upper area are at an angle of approximately 30°. In the latter these areas have obviously become so blended as to give a fairly uniform velocity direction.

The effective turning angle developed by various types of sills is summarized in Table V. It will be recalled that Equation (57) gave us an analytical approach to the part played by the sills in turning the water. The difference between the effective turning angle and the bend angle, θ , is supplied by the outside wall. Just what proper proportion of the total bend angle should be developed by the sills is a matter of considerable further research and is outside the scope of the present study.

TABLE V.

Comparison of Effective Angle of Turning for

Various Types of Sills

Sill Type	Discharge	P_y	P_x	ϕ
B	4.0	9.63	8.01	6.6°
	3.0	7.63	6.25	7.6°
	2.0	5.38	4.25	9.3°
C	4.0	7.56	6.50	4.5°
	3.0	6.00	5.19	5.9°
	2.0	4.56	3.38	7.8°
K	4.0	9.63	8.25	6.6°
	3.0	7.50	6.00	7.5°
	2.0	5.44	4.19	9.4°
I	4.0	10.13	7.76	7.0°
	3.0	7.63	6.19	7.6°
	2.0	5.63	4.13	9.7°
A	4.0	11.19	9.44	7.8°
	3.0	9.19	7.31	9.4°
	2.0	7.19	5.69	13.0°

V. CONCLUSIONS

A. SUMMARY OF RESULTS

This investigation has brought to light a means for controlling high-velocity flow around mild but abrupt bends in super-critically sloped open channels. The methods of control are the application of suitably-shaped and properly-dimensioned sills or low walls designed to repress the undesirable wave heights which exist in channels within and downstream from mild but abrupt bends. The sills should be placed echelon-fashion across the channel at the bend, the inside sill being omitted as it serves a negative purpose. The angle of the sills was found to be most effective when about three times the angle of the bend. Details of the best sill dimensions, arrangement and placement are given in Section III. B.

These corrective devices have the following advantages:

a. They reduce undesirable wave heights along the channel walls to small proportions.

b. They are self-cleaning.

c. They keep the flow of water in its super-critical state.

d. They are inexpensive to construct.

Their disadvantages are:

a. Their use is limited at present to bends of small angle.

b. Applied in flood channels, they would have to be replaced occasionally.

c. At low flows of water, the channel center might be subject to intermittent spraying (does not affect the walls)

The relative merits of these advantages or disadvantages will be discussed in the next section.

Fig. 6 is believed to be a chart which may hold the key to many future problems in super-critical flow. Careful analysis of observable and analytically-determined data led to the proposal of the explanation offered for its interpretation. It must be borne in mind that this explanation, before general adoption, should be experimentally investigated, such investigation having been foreign to the principal purpose of the present investigation. Experimental verification and research on this subject would probably also reveal the significance of the area in the lower right-hand corner of the chart. As a final presentation and summary of the effectiveness of the corrective devices proposed, Figures 68 through 75 are presented on the following pages, to show side by side the flow phenomena in the untreated channel and in the treated channel.

Fig. 68.
Untreated Channel

Fig. 69.
Treated Channel

Discharge = 4.0 cu.ft. per sec.

Fig. 70.
Untreated Channel

Fig. 71.
Treated Channel

Discharge = 3.0 cu.ft. per sec.

Fig. 72.

Fig. 73.

Discharge = 2.0 cu.ft. per sec.

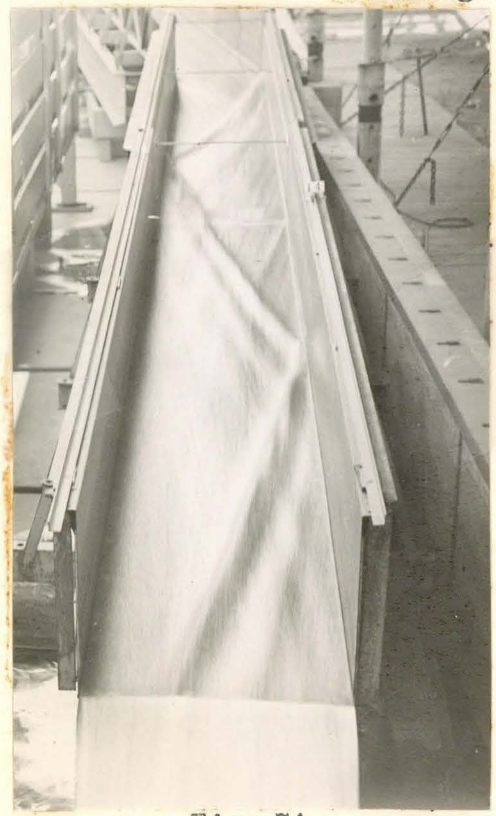

Fig. 74.

Fig. 75.

Discharge = 1.0 cu.ft. per sec.

B. APPLICATION TO FIELD CONDITIONS

The present findings can be applied to field conditions wherever the angle of the bend is small and the Froude number is such that the location on the chart of Fig. 6 is well to the left of the line marked "Locus of Minimum d_2/d_1". Sizes of sills, location within the channel, and transference of desired or anticipated results should be made in the usual manner, employing the Froude number as the governing criteria.

Disadvantages (b) and (c) listed in the preceding section are minor ones and relatively unimportant. Disadvantage (a), limitation to small bend angles, is listed as a disadvantage solely for the purpose of warning against its application in other than small bends. As pointed out in an earlier section, it is believed that this treatment might be applied to large angles by employing a series of small angle bends one downstream from another until the desired angle were attained. However, such application should first be thoroughly investigated, a research project in itself beyond the time and scôpe of this study.

The advantage of reductions in undesirable wave heights applied to flood channels means a much decreased wall height requirement at a correspondingly reduced cost. The self-cleaning characteristic is a requirement in any flood channel which might be required to carry debris. It is important to retain the flow in its critical state on a super-critically sloped channel because reduction to the sub-critical state is accompanied by an hydraulic jump of undesirable proportions. The treatment proposed, if properly applied, will keep the flow in its super-critical state.

BIBLIOGRAPHY

1. Knapp, Robert T. and Ippen, Arthur T. - "A Study of High Velocity Flow in Curved Sections of Open Channels" - An experimental and theoretical study carried out at the Hydraulic Structures Laboratory of the California Institute of Technology for the Los Angeles County Flood Control District, March, 1936.

2. Knapp, Robert T. and Ippen, Arthur T. - "Experimental Investigations of Flow in Curved Channels" - Research project for Los Angeles County Flood Control District, July, 1938.

3. Rouse, Hunter - "Fluid Mechanics for Hydraulic Engineers" - McGraw-Hill Book Co., 1938, pp. 283-4.

4. Kármán, Th. von - "Eine praktische Anwendung der Analogie zwischen Überschallströmung in Gasen überkritischer Strömung in offenen Gerinnen". Zeitschrift fur Angewandte Mathematik und Mechanik, Vol. 18, p. 49, 1938.

5. Rouse, Hunter - "A Method of Measuring High-Velocity Flow in Open Channels" - An investigation conducted for the Section of Watershed and Hydrologic Studies, USDA, SCS, Feb., 1939.

6. Rouse, Hunter - op. cit. 3 - pp. 399-401.

7. Rouse, Hunter - op. cit. 3 - pp. 369-370.

APPENDIX

A. LIST OF TABLES

APPENDIX

B. LIST OF FIGURES AND DRAWINGS

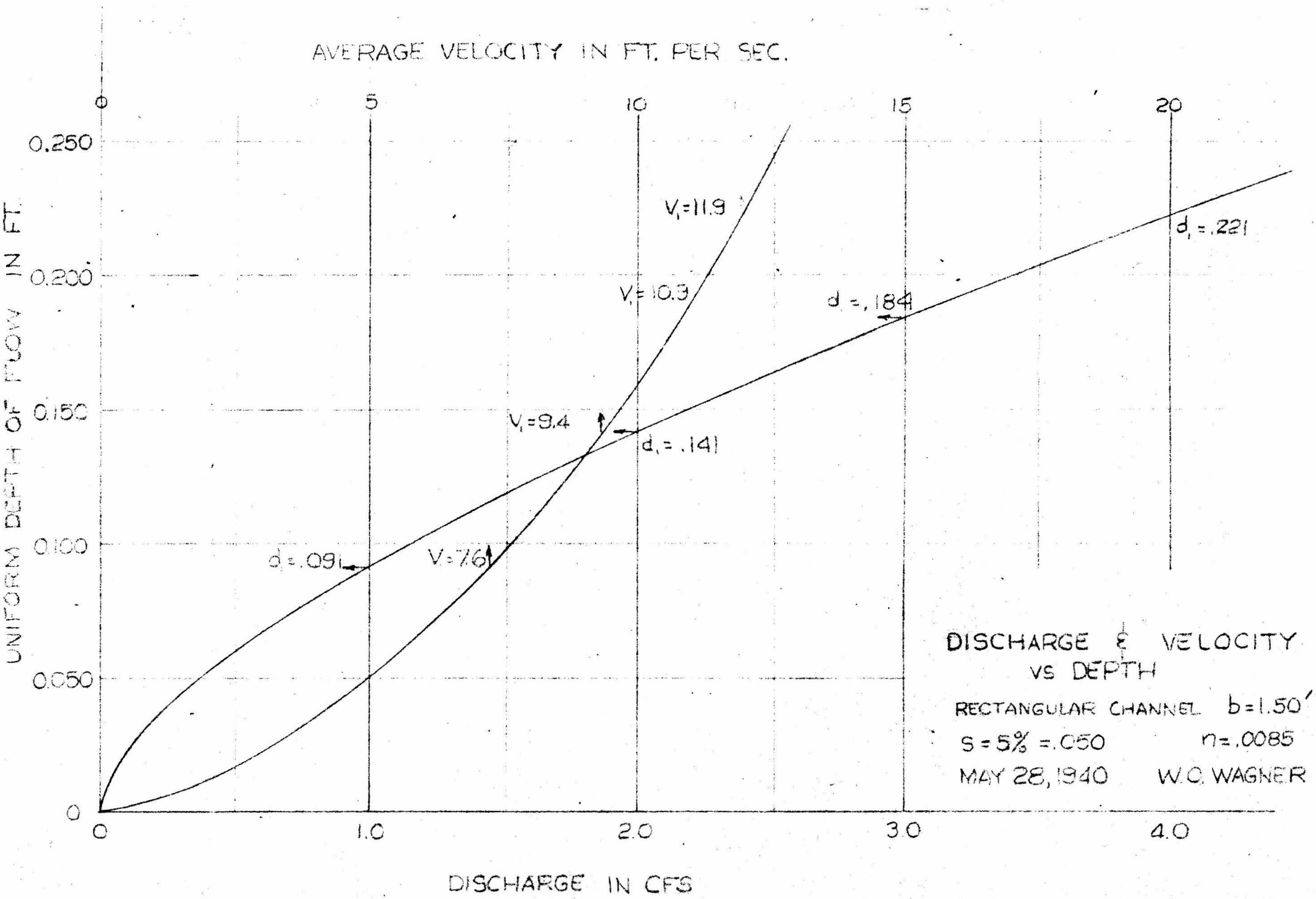

DISCHARGE & VELOCITY
vs DEPTH
RECTANGULAR CHANNEL b=1.50′
S = 5% = .050 n=.0085
MAY 28, 1940 W.C. WAGNER

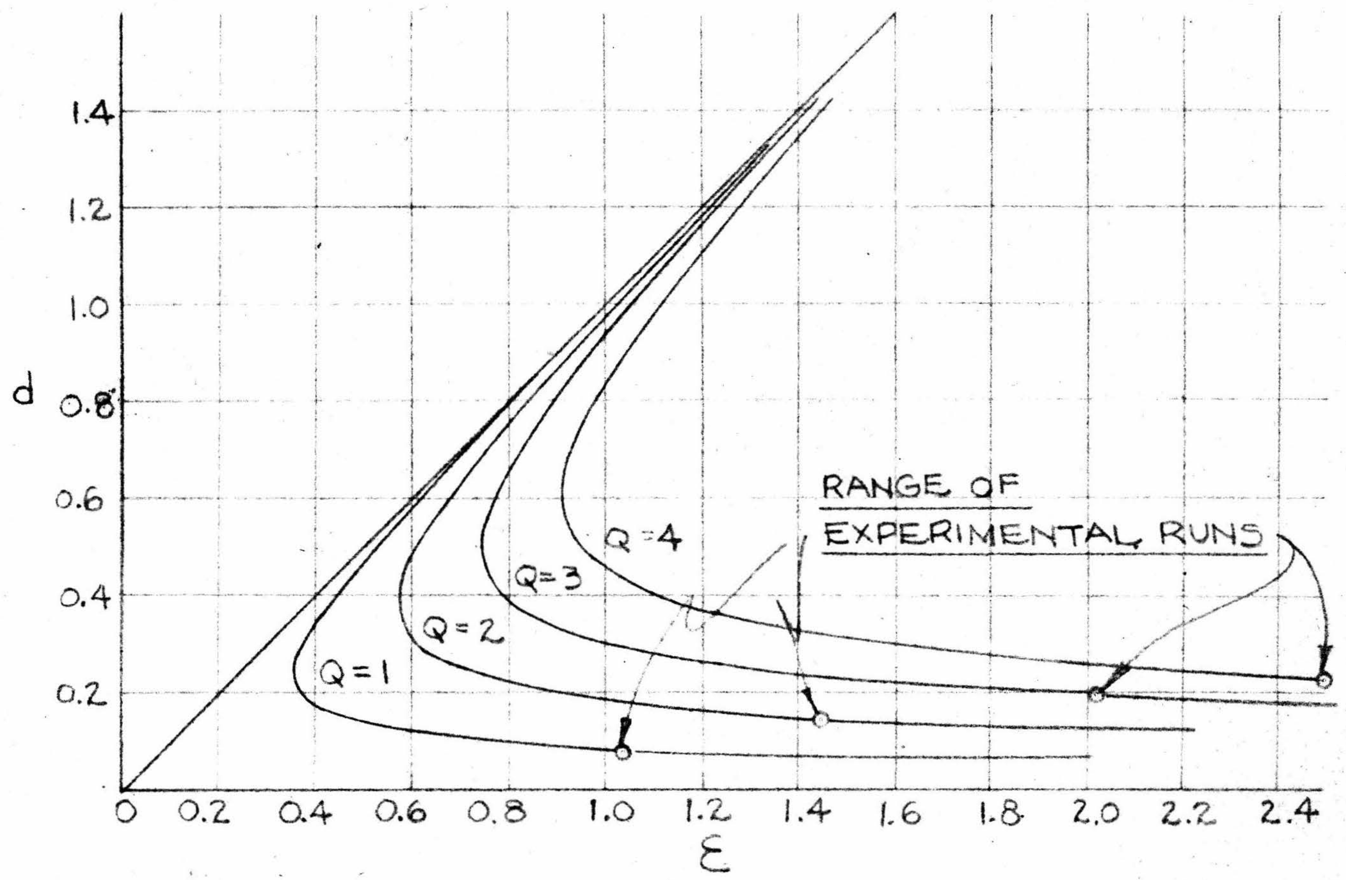

SPECIFIC ENERGY DIAGRAMS FOR
RECTANGULAR CHANNEL
b = 1.50 FT